Session 8

Refraction Modeling

Stefan Riepl, Erricos Pavlis

Some remarks on refractivity, raytracing and numerical weather models

Rüdiger Haas[1] and Stefan Riepel[2]

(1) Onsala Rymdobservatorium, Chalmers Tekniska Högskola, Göteborg (Sweden)

(2) Observatorio Tigo, Universidad de Concepcion, Concepcion (Chile)

Background (1)

- Refractive effects impact space geodetic measurements (optical and radio regime).
- The usual approach is to estimate ”zenith wet path delays” from the observational data themselves.
- This approach uses apriori mapping functions and the apriori modelling of dry/wet delays.

Background (2)

- The approach is quite good, but still a source of uncertainty, e.g. due to:

  a) Atmospheric inhomogenities.

  b) The strong correlation between station height, GM and zenith delays in SLR.

- Thus, a new modeling of zenith path delays is needed and should be developed.

Questions – Ideas

- Could apriori path delays (dry, wet) be modeled via raytracing through dense atmospheric fields?
- Could numerical weather models be used for this approach?
- Could atmospheric gradients be handeled?
- Could we completely skip estimating path delays in case this approach works?

Existing raytracing programs (1)

1) RayTrace

- Authors: Jim Davis (CfA Harvard), Tom Herring (MIT), Arthur Niell (MIT).
- Frequencies up to 300 GHz.
- Performs raytracing through vertical profiles, e.g. radiosonde profiles or numerical weather models.

Existing raytracing programs (2)

2) EGOPS

- Authors: G. Kirchengast et al. (Uni Graz).
- Licensed sofware, Fortran, IDL.
- Frequencies up to 1 THz.
- Liebe models for all gases.
- Performs 3D raytracing through 3D fields, e.g. standard atmospheres or numerical weather models.

Numerical weather models (1)

1) ECWMF

- Restricted access, some free.
- Interpolation to desired area and grid resolution possible, flexible (MARS archive).
- Pressure, temperature, humidity at several layers with 6 h time resolution.

Numerical weather models (2)

2) NCAR/NCEP

- Free access.
- Fixed grid size.
- Pressure, temperature, humidity at several layers with 6 h time resolution.

Numerical weather models (3)

3) e.g. MM5, HILAM

- Usually restricted access.
- Meteorological agencies, e.g. SMHI, DWD.
- Flexible grid resolution.
- Several levels with pressure, temperature, humidity.

Outlook

- Translating radio refractivity profiles from radio raytrace programs to the optical frequencies?
- Supplement existing radio raytrace progams with code for optical frequencies?
- Developing a completely new optical raytrace program?

Low Elevation Data Analysis
Grasse (7845)

Erricos C. Pavlis

Magda Kuzmicz-Cieslak

JCET/UMBC - NASA/GSFC

2003 ILRS Workshop on Laser Ranging
October 28-31, 2003, Kötzting, Germany

Introduction

- Analyzed data span:
  - October 21, 2001 to December 15, 2002
  - January 12, 2003 to February 7, 2003
- Data come from a single site:
  - **Grasse, 7845**
- Data were deposited in the form of full rate data on the EDC archive, under a separate directory

Analysis

- The data were reduced using the orbital model fit to the standard weekly data sets
- A measurement bias for Grasse was simultaneously estimated since it was apparent that the data were biased at about the 2 cm level

Analysis (cont.)

- Atmospheric refraction corrections were applied in two different ways:
  - standard Marini - Murray model **[MM]**
  - a variation of Ciddor's ZD model by Mendes and the new FCUL (Mendes et al.) mapping function **[MC]**
- Residual differences examined for data below $\varepsilon < 10°$

Residual Differences vs. Elevation

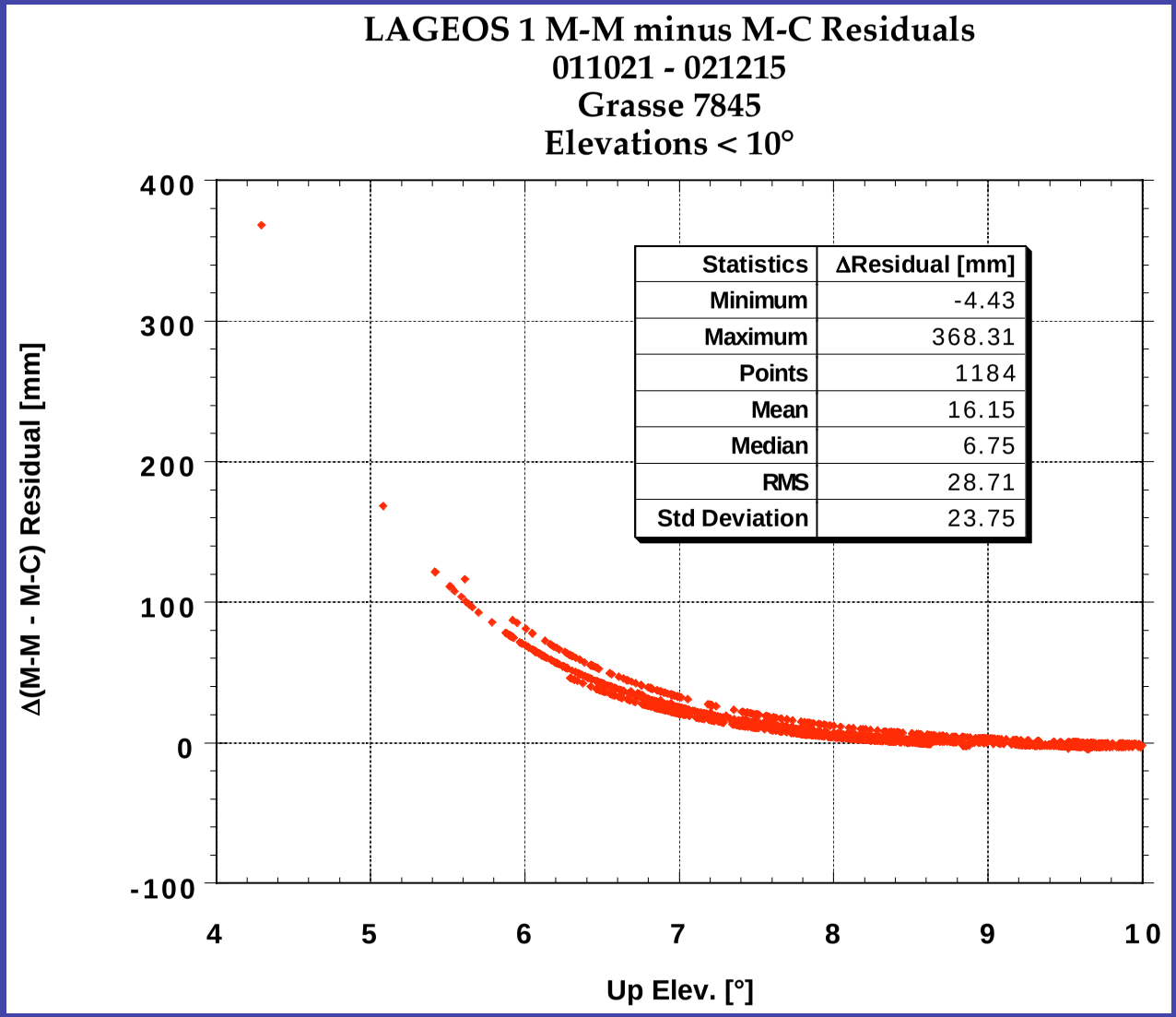

Residual Differences vs. Elevation

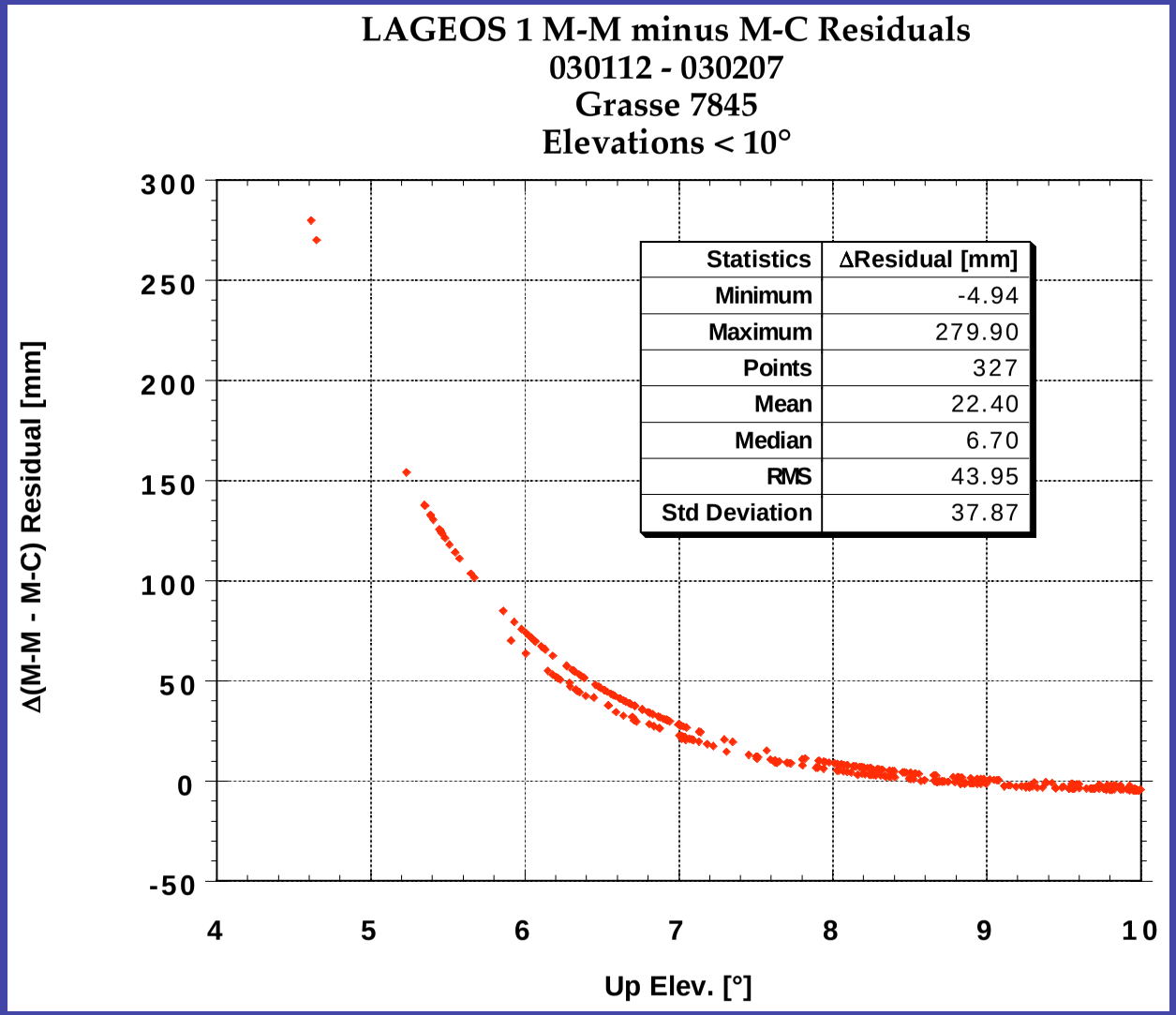

Residual Differences vs. Elevation

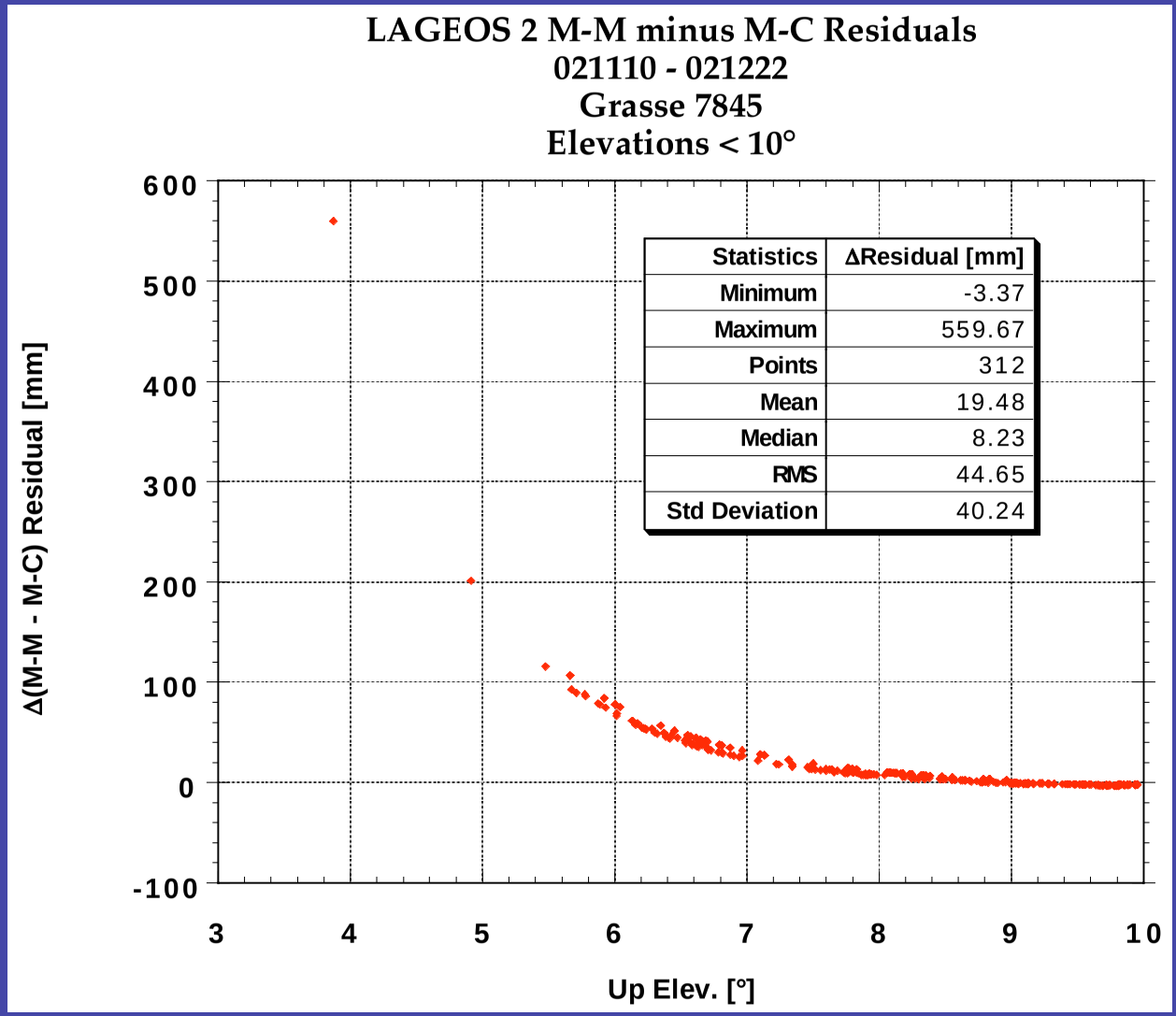

Residual Differences vs. Elevation

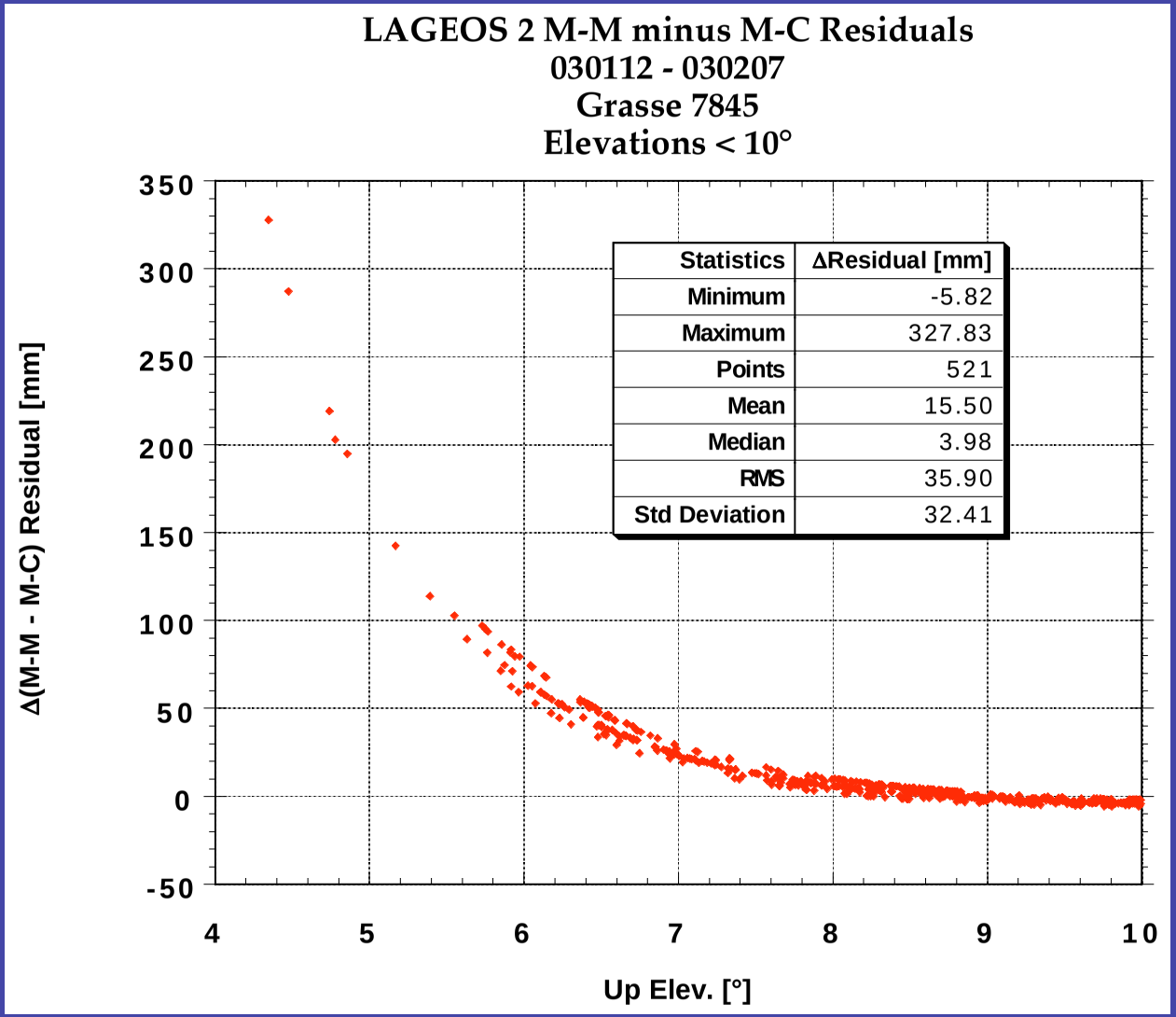

MM vs. MC

LAGEOS 1 & 2 Residual Statistics MM and MC Models

LAGEOS 1

Marini - Murray

	M-M Residual [m]
Minimum	-0.0537
Maximum	0.1872
Points	327
Mean	0.0504
Median	0.0402
RMS	0.0669
Std Deviation	0.0441

Mendes - Ciddor

	M-C Residual [m]
Minimum	-0.1266
Maximum	0.0965
Points	327
Mean	0.0280
Median	0.0276
RMS	0.0368
Std Deviation	0.0240

LAGEOS 2

	M-M Residual [m]
Minimum	-0.0666
Maximum	0.1607
Points	516
Mean	0.0345
Median	0.0333
RMS	0.0536
Std Deviation	0.0411

	M-C Residual [m]
Minimum	-0.1217
Maximum	0.1282
Points	516
Mean	0.0212
Median	0.0203
RMS	0.0442
Std Deviation	0.0388

Summary

- The system seems to deliver substantial data down to about 5° elevation
- The results indicate that applying M-M in the analysis for low elevation data ($5° < \varepsilon < 10°$) will introduce a mean bias of about 5 cm
- This will artificially increase the residual scatter for that site, but even worse, it will bias the recovered position of that site

Conclusions

- The system seems to deliver substantial data down to about 5° elevation
- Residual differences between reductions based on the M - M vs. those using the M - C increase exponentially with decreasing elevation, reaching several centimeters
- We need more low elevation data from many more systems, even if that data comes from lower (“clean”) geodetic targets (e.g. Starlette)

Atmospheric absorption lines and nonlinear refractivity of air effects.

Yury Galkin
Moscow State Forest University
(1, 1st Institutskaya St., Mytischi-5, Moscow reg., 141005, Russia,
tel. 7-095-786-1442, fax 7-095-586-9134, e-mail galkin@mgul.ac.ru)
and

Ruben Tatevyan
Central Scientific Research Institute
of Geodesy, Aerosurvey and Cartography
(26, Onezhskaya St., Moscow, 125413, Russia,
tel. 7-095-456-9321,)

Presented at the
International Laser Ranging Workshop
October 28-31, 2003
Koetzting, Germany

Introduction. The modern state of the art position.

It is known that the XXII General Assembly in 1999 recommended TWO formulas for the refractive index of the atmosphere suggested by the Ad-Hoc Working Group "Refractive indices of light, infrared and radio waves in the atmosphere" (Rueger (2002)). One of them (in Taylor's series form) is low accuracy (1 ppm), another (in Sellmeier's form) is more accuracy (better 1 ppm). State-of-the- art dispersion formulas are based on UV continium effect only. Usually exact formulas may be written, as follow

$$N \cdot 10^8 = (n - 1) \cdot 10^8 = A + \frac{B}{C - \sigma^2} + \frac{D}{E - \sigma^2}$$

where the coefficients A,B,C,D,E were suggested by different authors and the best of them is shown in table 1.

Table 1. The coefficients are suggested by different authors.

	A	B	C	D	E	
1.	Given as Taylor's series					Recommended by the XXII GA (1999)
2.	0	5792105	238,0185	167917	57,362	Recommended by the XXII GA (Ciddor96)
3.	8060,51	2480990	132,274	17455,7	39,329957	Peck&Reeder (1972) formula
4.	8342,13	2406030	130	15997	38,9	**Edlen's (1965) formula**
5.	8629,574	2323732,3	127,060012	12989,105	37,884361	**Galkin and Tatevyan (1997) formula**

The last experimental data were written by Peck and Reeder (1972) which have corrected some experimental data of Peck and Khanna (1962) (about $0.5 \bullet 10^{-8}$) and fitted new data to obtain new dispersion formula. Unfortunately anything special experimental data is absent and the XXII GA recommended two formulas (low precision and high precision) grounded by Peck and Reeder analysis and corrected on the temperature scale and CO2 content. Results of comparing are shown in the Table 2

Additionally there is shown optimized formula, which has the lowest RMS in last column.

Table 2. The differences of the formulas calculations minus the experimental data

—	**Wavelength □ micrometers**	**$N_{experim}$ x10E-8**	**Recommended as easy formula by the XXII GA (1999)**	**Recommended as exact formula by the XXII GA (Ciddor96)**	**Peck&Reeder (1972) formula**	**Edlen's (1965) formula**	**Galkin and Tatevyan (1997) formula**
1	1,694521	27314	4,1541956	1,5445055	0,2655215	0,7167135	0,2738517
2	1,530015	27326,41	4,0082396	1,3113552	0,0200432	0,4603064	0,0212895
3	1,529977	27326,1	4,3215394	1,6246317	0,3333165	0,7735767	0,3345609
4	1,529354	27326,56	3,9156752	1,2183842	-0,0729843	0,3672279	-0,0717708
5	1,47565	27331,28	4,1244603	1,3923415	0,0961548	0,532007	0,0945681
6	1,372233	27342,34	4,2468603	1,4362005	0,1293671	0,555395	0,1215256
7	1,372233	27342,52	4,0668603	1,2562005	-0,0506329	0,375395	-0,0584744
8	1,350788	27345,38	3,8548095	1,0256513	-0,2836459	0,1400694	-0,2929485
9	1,350788	27345,31	3,9248095	1,0956513	-0,2136459	0,2100694	-0,2229485
10	1,12905	27381,47	4,6740507	1,5913565	0,2499526	0,6419776	0,2210678
11	1,014257	27410,87	4,668668	1,3904036	0,026322	0,393831	-0,0171248
12	1,014257	27410,78	4,758668	1,4804036	0,116322	0,483831	0,0728752
13	0,966043	27426,28	4,8768434	1,49721	0,1220833	0,4768247	0,0712656
14	0,922703	27442,66	4,7030755	1,2202605	-0,1656118	0,1760694	-0,2238127
15	0,912547	27446,62	4,8828814	1,3740496	-0,0144528	0,323923	-0,0744967
16	0,912547	27446,43	5,0728814	1,5640496	0,1755472	0,513923	0,1155033
17	0,724716	27557,42	5,4666071	1,3171648	-0,1256837	0,1283708	-0,2289407
18	0,671829	27606,4	6,2493796	1,8564568	0,398697	0,6179052	0,2799573
19	0,644025	27638,2	5,7908657	1,2602317	-0,2042629	-0,0061245	-0,3315975

Table 2. The differences of the formulas calculations minus the experimental data

—	Wavelength □ micrometers	$N_{experim}$ x10E-8	Recommended as easy formula by the XXII GA (1999)	Recommended as exact formula by the XXII GA (Ciddor96)	Peck&Reeder (1972) formula	Edlen's (1965) formula	Galkin and Tatevyan (1997) formula
20	0,579226	27729,8	6,1029558	1,2464663	-0,2271617	-0,0869784	-0,3747713
21	0,57712	27733	6,4360516	1,5695381	0,0958489	0,2339169	-0,0523982
22	0,567747	27749,7	5,956003	1,0459983	-0,4277184	-0,2992559	-0,5787617
23	0,546227	27789,88	6,3382817	1,3382644	-0,1337797	-0,0285848	-0,2908928
24	0,501707	27891,53	6,4743271	1,3759449	-0,0822914	-0,0308325	-0,249099
25	0,49233	27916,71	6,4789896	1,3866325	-0,0663735	-0,0272043	-0,234421
26	0,491745	27918,7	6,1101503	1,0186167	-0,4340312	-0,3956395	-0,6021433
27	0,471446	27978,61	6,4204893	1,3982244	-0,0394525	-0,0288066	-0,2087149
28	0,467946	27989,85	6,401085	1,4002925	-0,0342683	-0,0285487	-0,2034821
29	0,447273	28062,08	6,1869999	1,391607	-0,0209681	-0,0450807	-0,1880079
30	0,435956	28106,3	6,0364431	1,4270908	0,0293266	-0,0115419	-0,1348728
31	0,435956	28106,5	5,8364431	1,2270908	-0,1706734	-0,2115419	-0,3348728
32	0,410933	28218,4	5,4107101	1,4926233	0,1349515	0,0566276	-0,0174304
33	0,404771	28249,54	5,1390278	1,4716239	0,1253279	0,0378494	-0,0227096
34	0,404771	28249,5	5,1790278	1,5116239	0,1653279	0,0778494	0,0172904
35	0,398509	28282,8	4,8201513	1,4501186	0,1159236	0,0192436	-0,0270109
36	0,388975	28336,79	4,2754431	1,4556653	0,140781	0,030398	0,0070821
37	0,380273	28390,5	3,1408789	0,9474014	-0,3492042	-0,4716177	-0,4727619
38	0,365587	28489,6	2,0698116	1,2815469	0,0159162	-0,1252089	-0,0863247
39	0,365119	28492,9	2,1040497	1,369229	0,104561	-0,0371174	0,0030936
40	0,356224	28559,5	1,5906434	1,9949496	0,7478589	0,5963095	0,6622768
41	0,354443	28574,4	0,5710811	1,2343384	-0,0094555	-0,1628165	-0,0915788
42	0,339168	28705,9	-1,9908321	1,4205045	0,1996018	0,0335988	0,1511246
43	0,29263	29264,3	-21,125423	1,5153873	0,1900421	0,0430504	0,2786222
44	0,289447	29314,4	-23,487773	1,5428644	0,1912606	0,0507216	0,2889381
45	0,285779	29374,8	-26,660677	1,3992657	0,0128765	-0,1190613	0,1202801
46	0,276059	29548,7	-36,385156	1,404872	-0,0984449	-0,2008539	0,0284199
47	0,27536	29562,1	-37,222981	1,377451	-0,1356618	-0,2355349	-0,0078913
48	0,267575	29719,8	-47,443707	1,4072727	-0,2259716	-0,2934173	-0,0947281
49	0,257711	29945,5	-64,119415	1,7180661	-0,0819116	-0,0959524	0,0284762
50	0,246482	30245,7	-90,652656	2,20108	0,2740376	0,3407201	0,3034355
51	0,244765	30297,3	-96,565969	1,3659913	-0,5614117	-0,480221	-0,5519836
52	0,237911	30514,4	-119,81141	1,6075054	-0,2099204	-0,0640882	-0,3062783
53	0,234617	30628,3	-133,49383	1,3558144	-0,3098704	-0,1286014	-0,4739523
54	0,230289	30787,6	-153,46746	1,5999116	0,2944622	0,5276015	0,0227756
55	0,214506	31496,8	-267,91322	-3,9468422	-0,2064336	0,3096475	-1,0080198
56	0,202605	32214,8	-423,92365	-17,189431	2,5912883	3,6500984	1,8825077
57	0,199052	32479,5	-497,03363	-31,113787	-1,0207661	0,3833109	-1,1874386
58	0,193585	32939,7	-637,244	-58,775678	-2,2454354	0,1255087	-0,1200724
59	0,186277	33697,4	-912,5541	-127,39999	5,2981688	11,109373	18,363192
60	0,185473	33805,5	-963,30413	-150,25495	-4,0859011	2,4234463	11,406945
			±124.499	**±9.199**	**±0.524**	**±0.554**	**±0.404**

In whole experimental data confirmed dispersion formula but however some experimental measurements (very high precision) gave more high magnitude for some wavelengths.

Table 3. Some experimental results after 1972

_	Authors	Range micrometers	Method	Data - Ed.65 in 10^{-8}
1	Schellekens et al (1986)	0.63	NPL	+6.0
2		0.63	PTB	+0.1
3		0.63	THE	+8.0
4		0.63	VSL	+3.0
5	Matsumoto (1988)	10	Michelson	+5.0
6	Birch and Downs (1993)	0.63	NPL	+5.9
7	Hou and Thalmann (1994)	0.63	OFMET	+1.4
8		0.63	BCR	+3.4

This situation and some former results (two color refractometer, IR EDM) gave the idea that special reasons may be here.

Influence of the atmospheric absorption lines.

It is known that there are a lot of (more 1000000 by the HITRAN electronoc basedata) resonances (absorption lines) from IR to RW. In generaly the resonances are combined by groups (absorption bands) including 100s or even 1000s separated absorption lines.
Usually a single absorption line near of the earth surface has the Lorentian form

$$\alpha(\nu) = \frac{S_i c}{2\pi_i} N \frac{g^2 \pi_i^2}{(\nu - \nu_i)^2 + g^2 \pi_i^2} = AN \frac{g^2 \pi_i^2}{(\nu - \nu_i)^2 + g^2 \pi_i^2}$$

Therefore change of the phase refractive index because of absorption may be written as

$$n(\nu) - 1 = ANg \frac{S_i(\nu_i - \nu)}{(\nu_i - \nu)^2 + \pi_i^2 g^2}$$

Symbolic graph shows resulting “unsmooth” curve.

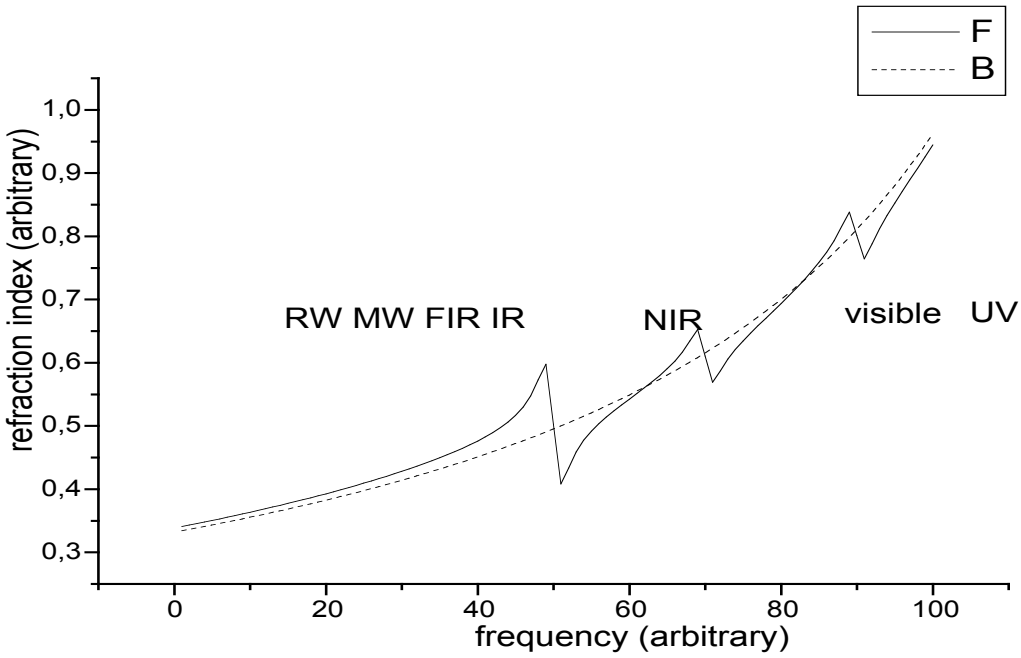

A single line has small effect 10^{-9}- 10^{-12} on the phase refractive index. This effect on short wave side aspires to zero, but (warning) one on long wave side aspires to a fixed terminal value. Therefore, the refractive index on long wave side of absorption band is above (sum of all lines effect) then the UV effect curve. We can acount important bands of the general atmospheric components (O_2, H_2O, CO_2 etc.) within visible, NIR, MIR, FIR and RW regions. The real refractive index of air is more complicated then the known formulas show.
More than that the group refractive index near absorption line may be written as

$$n_{gr}(\nu) - 1 = AN\gamma \frac{2(\nu_i - \nu)^3\gamma^2 + \gamma_i^2(\nu_i - \nu)^2 - \gamma_i^4\gamma^2}{\left[(\nu_i - \nu)^2 + \gamma_i^2\gamma^2\right]^2}$$

And if we take

$$x = \frac{\nu_i - \nu}{\gamma\gamma_i} \qquad \text{where} \quad \gamma\gamma_i \text{ is the halfwidth of the i-line}$$

we can easily estimate region of influence every line in number of the halfwidth of the line

$$\alpha(x) = AN\frac{1}{1+x^2} \qquad n(x) - 1 = AN\frac{x}{1+x^2} \qquad n_{gr}(x) - 1 = \frac{AN(x^2-1)}{\gamma(1+x^2)^2}$$

Usually AN is 10^{-9}-10^{-12} and g $\approx 10^{-6}$ for visible and IR regions therefore the single line effects on the group refractive index is million times more than on the phase index within spectral region from 0,5 nm to 50 nm around of a signal carrier frequency.
The phase refractive index is destroyed just when the signal spectrum and the absorption line are intersecting.
Since the SLR uses the group refractive index there are shown number of lines within of the ± 5 nm range around of the laser wavelengths used by SLR in Table 4.

Table 4. Absorption lines near SLR wavelengths.

No	Laser wavelength micrometer	O_2	CO_2	H_2O	The nearest line
1	0,353	Outside of database			
2	0,4235	0	0	0	0
3	0,435	0	0	0	0
4	0,46	0	0	0	0
5	0,532	0	0	32	0,5325
6	0,6329	85	0	117	0,632908
7	0,6942	124	0	218	0,69421
8	0,683	38	0	65	0,68304
9	0,847	0	0	105	0,847005
10	1,064	51	34	21	1,06402
11	1,57	17	232	36	1,570003

It is seen that in most cases the state of the art smooth dispersion formula is not enough for precision group refractive index of the air and real dispersion is not known and the special researches are required.
More than that, the oscillating form of the dispersion may be as reason of breach of correction of the group refractive index formula in whole.

Nonlinear refractivity effects.

The XXII General Assembly recommended to use the group refractive index calculated using the computer procedure suggested Ciddor and Hill (1999). This procedure assumes that the conditions are realized in air may be written as following

$$\square(\square_0) \square \square 0.5 \square(\square_0) \square^2$$

When the properties of medium (absorption and refractivity) may be written as the Taylor's series of the complex function

$$\square(\square_0)\square\square\square(\square_0)\square$$

$$k(\square) = k(\square_0) + k\square(\square_0)\square + 0.5k\square\square(\square_0)\square^2 + \ldots =$$
$$= \square(\square_0) + \square\square(\square_0)\square + 0.5\square\square\square(\square_0)\square^2 + \ldots$$
$$+ i\square(\square_0) + i\square\square(\square_0)\square + i0.5\square\square\square(\square_0)\square^2 + \ldots$$

where $k(\square)$ is a complex vector in a Taylor series in powers of $\square=(\square\square\square_0)$ for the absorption coefficient $\square(\square)$ and the phase delay $\square(\square)$

Unfortunately above-mentioned conditions may be not executed near absorption lines even for simple signals (AM-signal) (Galkin and Tatevyan (1997)). These conditions are destroyed even far away from absorption lines for the complicated signals, for example, such as the short laser pulse with the Gaussian envelope (width $\square$ at 50% power) (Galkin and Tatevyan (2002)). In this case using of the state of the art group refractive index gives an error in results because of the nonlinear refractivity gives the additional group delay

$$\square = \frac{2.78\square^2\square\square\$^2}{1+2.78\square^2\square\$}$$

and the shift received frequency relatively of transmitted optical frequency approximately as

$$\square\square = \square 2.78\square^2\square\$$$

where S is path through atmosphere, and the necessary derivatives can be calculated by Kramers-Kronig relations using known dispersion function (for the derivatives of absorption) or transparency function (for the derivatives of refraction).

The estimation of the additional group delay and the frequency shift for the state of the art dispersion equation and different laser wavelengths is shown on the Table 5. (Sensing to zenith. S=16,6 km)

Table 5. The additional group delay and the frequency shift for used lasers.

Wavelength micrometers	Pulse width 1 nsec		Wavelength micrometers	Pulse width 0,1 nsec	
	psec	$\times 10^{10}$		psec	$\times 10^{12}$
1,57	0,003	1,5	1,57	0,257	1,5
1,06	0,006	2,4	1,06	0,601	2,4
0,85	0,01	3,2	0,85	1,009	3,2
0,69	0,017	4,3	0,69	1,678	4,3
0,53	0,034	6,5	0,53	3,353	6,5
0,42	0,061	9,6	0,42	6,081	9,6
0,35	0,115	14	0,35	11,42	14

The additional group delay is the most important aspect for two color SLR. For two color measurements (Sperber and Riepl (2001)) the atmospheric correction may be obtained via the time delay Δt the pulses of different color (let $\lambda_1<\lambda_2$)

$$N_{gr}(\lambda_1)\, S = cN_{gr0}(\lambda_1)\, \Delta t\, (N_{gr0}(\lambda_2) - N_{gr0}(\lambda_1))^{-1}=cK\Delta t$$

where the components $N_{gr0}(\lambda_1)$ and $N_{gr0}(\lambda_2)$ are known and the factor K may be calculated, c is the light velocity in vacuum. According to this factor influence of the additional delay is increasing.

The resulting errors are calculated for a vertical ray path (double ray path through at sea level is assumed as 16.6 km) and a horizontal ray (path is equal 50 km) for different conditions. They are shown in Tables 6 – 9.

Table 6. Vertical ray path. Pulse width is 1.0 nsec.

$\lambda\lambda$(μm)	$\Delta\Delta$ (psec)	K	Error (mm)
1.064-0.532	0.027	22.6	0.18
0.532-0.355	0.077	14.06	0.32
1.064-0.355	0.10	8.44	0.26

Table 7. Vertical ray path. Pulse width is 0.1 nsec

$\lambda\lambda$(μm)	$\Delta\Delta$ (psec)	K	Error (mm)
1.064-0.532	2.72	22.6	18.44
0.532-0.355	7.68	14.06	33.64
1.064-0.355	10.4	8.44	26.33

Table 8. Horizontal ray path. Pulse width is 1.0 nsec.

□□(□m)	□□ (psec)	K	Error (mm)
1.064-0.532	0.30	22.6	2.02
0.532-0.355	0.69	14.06	2.91
1.064-0.355	0.99	8.44	2.50

Table 9. Horizontal ray path. Pulse width is 0.1 nsec

□□(□m)	□□ (psec)	K	Error (mm)
1.064-0.532	24.5	22.6	166.11
0.532-0.355	69.1	14.06	237.0
1.064-0.355	93.6	8.44	302.7

Conclusions

It is shown that the state of the art dispersion formulas particularly of the group refractive index is not enough to achieve millimeter accuracy of the SLR.
Taking into consideration a lot of the spectral lines of air it is necessary to research every used spectral region in detail by theoretic and experimental methods.
Worth while to pay attention on stated problems under exploitation of the existing SLR systems and development new perspective ones.

References.

Birch K.P., Downs M.J. (1993) Metrologia, v.30, p. 155.
Ciddor P.E. (1996) Applied Optics, Vol. 35, No. 9, 1566-1573.
Ciddor P.E., Hill R.J. (1999) Applied Optics, Vol. 38, No. 9, 1663-1667.
Edlen B. (1966) Metrologia, v.2, p. 71.
Galkin Yu.S., Zakharov D., Tatevian R.A. (1997) Geodesy and Cartography, No 11 (in Russian).
Galkin Yu.S., Tatevian R.A. (1997) Journal of Geodesy, No 71, 483-485.
Galkin Yu.S., Tatevian R.A. (2002) Presentation at the 13th ILRS, Washington D.C., USA.
Hou W., Thalmann R. (1994) Measurements, v.13, p. 307.
Mutsumoto H. et al. (1988) Metrologia, v. 25, p. 95.
Peck E.R., Khanna B.N. (1962) JOSA, v.52, p. 416
Peck E.R., Reeder K. (1972) JOSA, v.62, p. 958.
Rüeger J. M. (2002) UNISURV REPORT S-68, School of Surveying and Spatial Information Systems, University of New South Wales, Sydney, Australia.

Schellenkens P. et al. (1986) Metrologia, v.22, p. 279.
Sperber P., Riepl S. (2001) Proc. of the Int. conference “Mathematical and physical methods in ecology and environmental monitoring”, Moscow, Russia, 30-43.

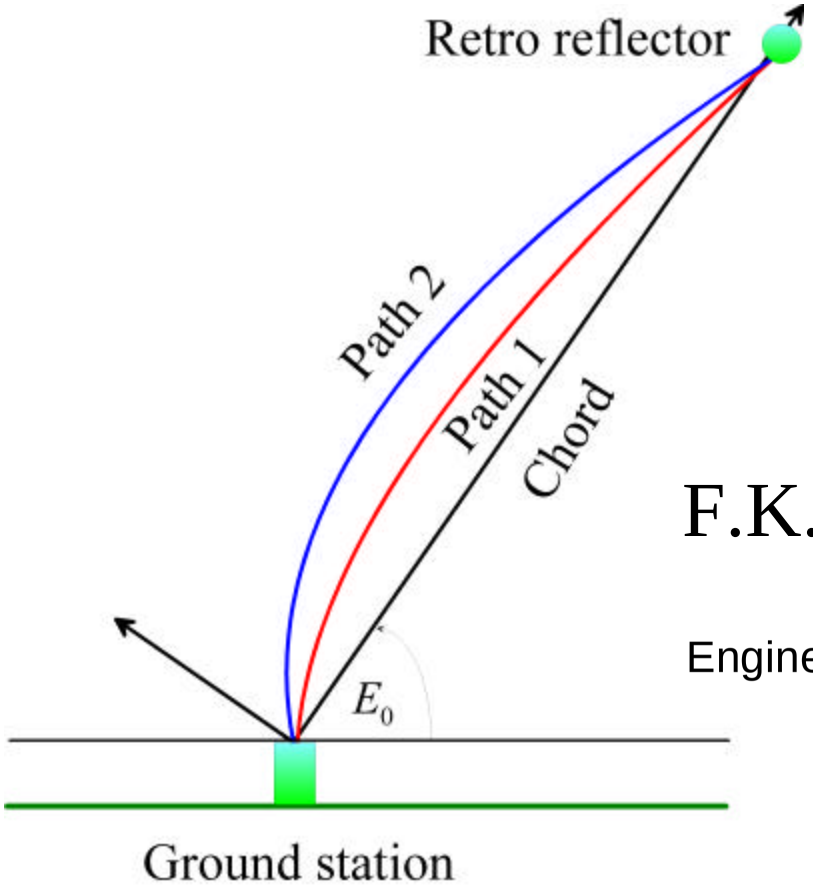

Modelling of dual-wavelength SLR measurements

F.K. Brunner and K.H. Gutjahr

Engineering Geodesy and Measurement Systems
Graz University of Technology

Motivation

Contribution to

Refraction Study Group (RSG) of ILRS

Goal was set to achieve

$$s_s \cong 1mm$$

Rigorous derivation of atmospheric effects in dual-wavelength SLR

Rigorous Derivation (1)

- Integration path determined by n_{ph}
- OPL = integration of n_{gr} along path yielding L_1 and L_2

$$L_1 = s + \int_{path1} \left[n_{gr}(l_1) - 1 \right] \cdot ds_1 + K_1$$

$$L_2 = s + \int_{path2} \left[n_{gr}(l_2) - 1 \right] \cdot ds_2 + K_2$$

$$L_2 = s + \int_{path1} \left[n_{gr}(l_2) - 1 \right] \cdot ds_1 + K_1 + P$$

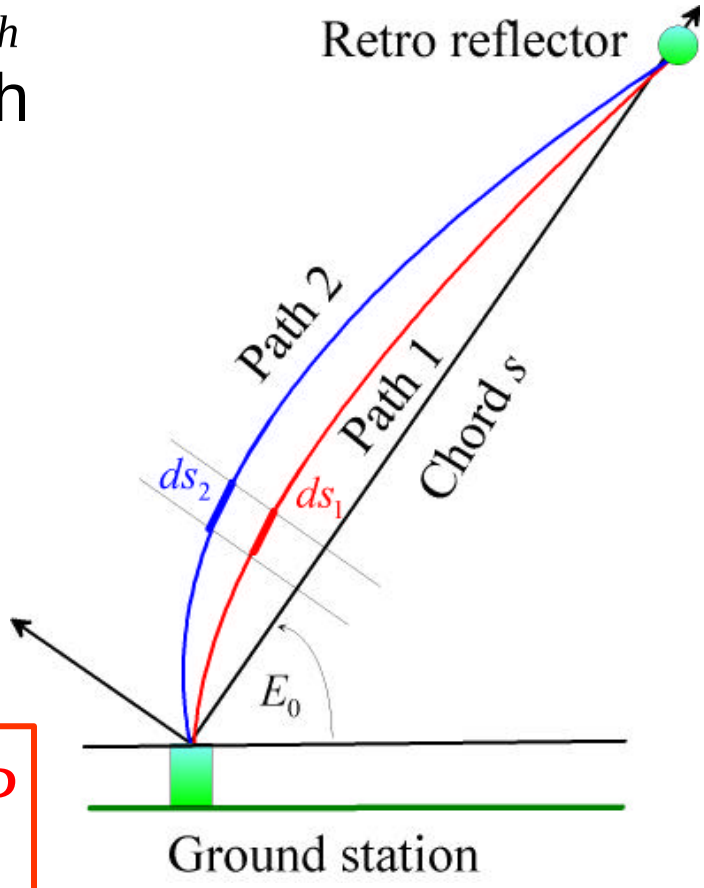

Rigorous Derivation (2)

- n_{gr} is expressed by dispersion factors and the associated densities of air

$$n_{gr} = 1 + D(l)\, r_{dry} + W(l)\, r_{wet}$$

- This leads to

$$L_1 = s + D(l_1) \int_{path1} r_{dry} \cdot ds_1 + W(l_1) \int_{path1} r_{wet} \cdot ds_1 + K_1$$

$$L_2 = s + D(l_2) \int_{path1} r_{dry} \cdot ds_1 + W(l_2) \int_{path1} r_{wet} \cdot ds_1 + K_1 + P$$

- Now $\int_{path1} r_{dry} \cdot ds_1$ can rigorously be eliminated

Rigorous Derivation (3)

$$s = L_1 - n\left(L_2 - L_1\right) + \left(nP - K_1\right) + W\left(l_1\right) H_{12} \int_{path1} r_{wet}\, ds_1$$

$$n \equiv \frac{D\left(l_1\right)}{D\left(l_2\right) - D\left(l_1\right)}$$ ... dispersive power

$$H_{12} \equiv \frac{W\left(l_2\right) - W\left(l_1\right)}{W\left(l_1\right)} - 1$$ ... humidity reduction factor

Raytracing

- Snell´s law
- Spherical layers of atmosphere of 1 m thickness
- 1976 Standard atmosphere values for temperature and pressure

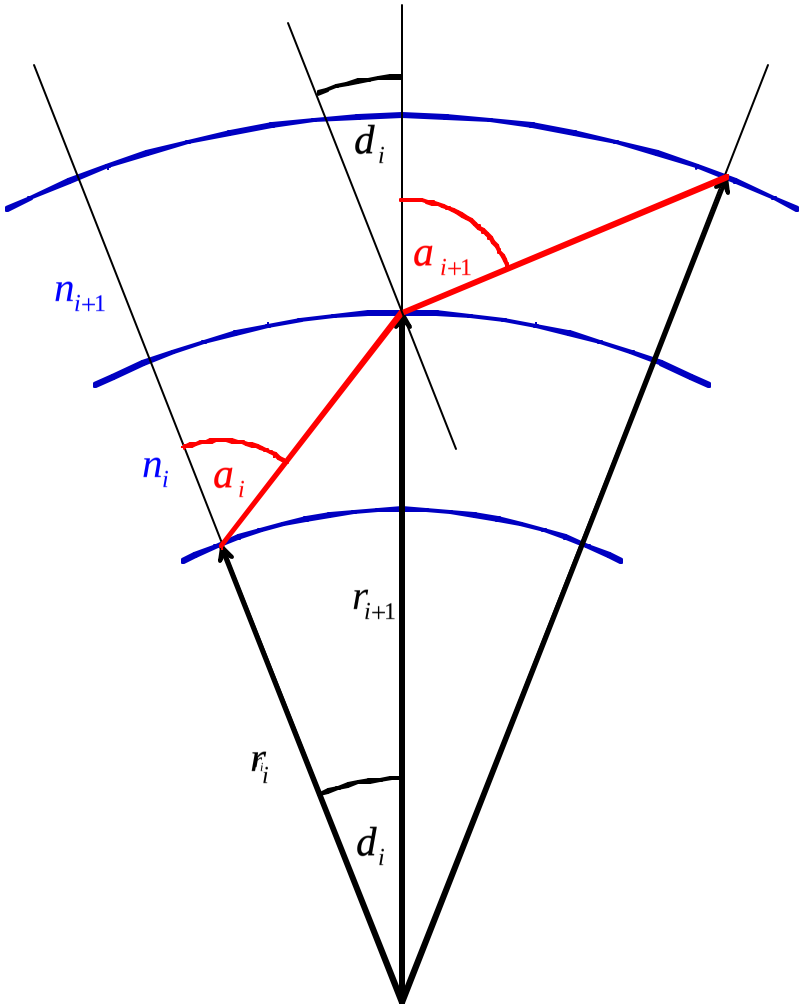

1976 Standard Atmosphere

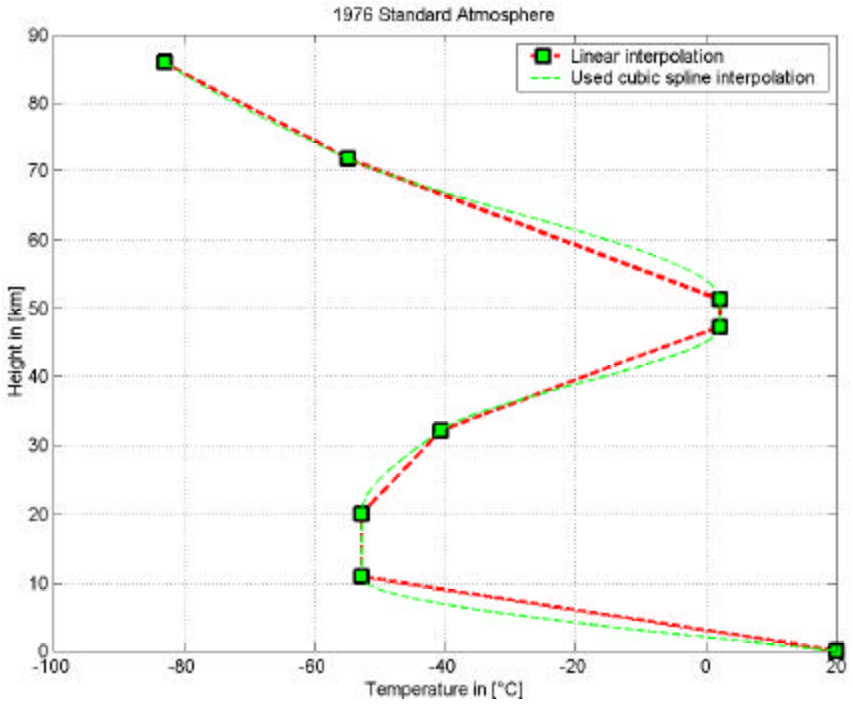

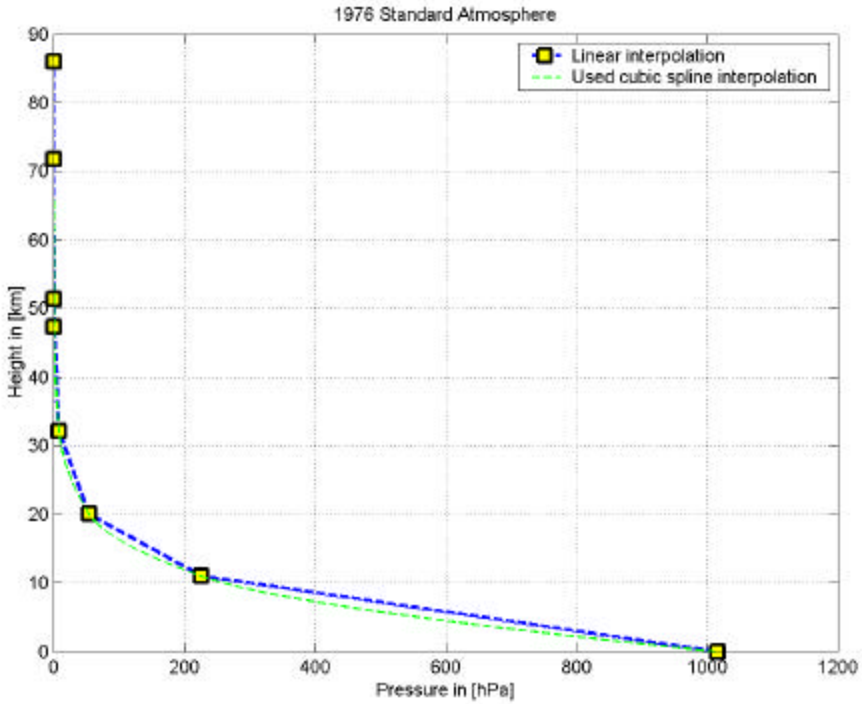

- Defined up to 86 km
- Start values at sea level: 20° C and 1016 hPa

Curvature and Propagation Effect

Curvature $$K_1 = \int_{path1} ds_1 - s$$

Propagation $$P = \int_{path2} n_{gr}(l_2) \cdot ds_2 - \int_{path1} n_{gr}(l_2) \cdot ds_1$$

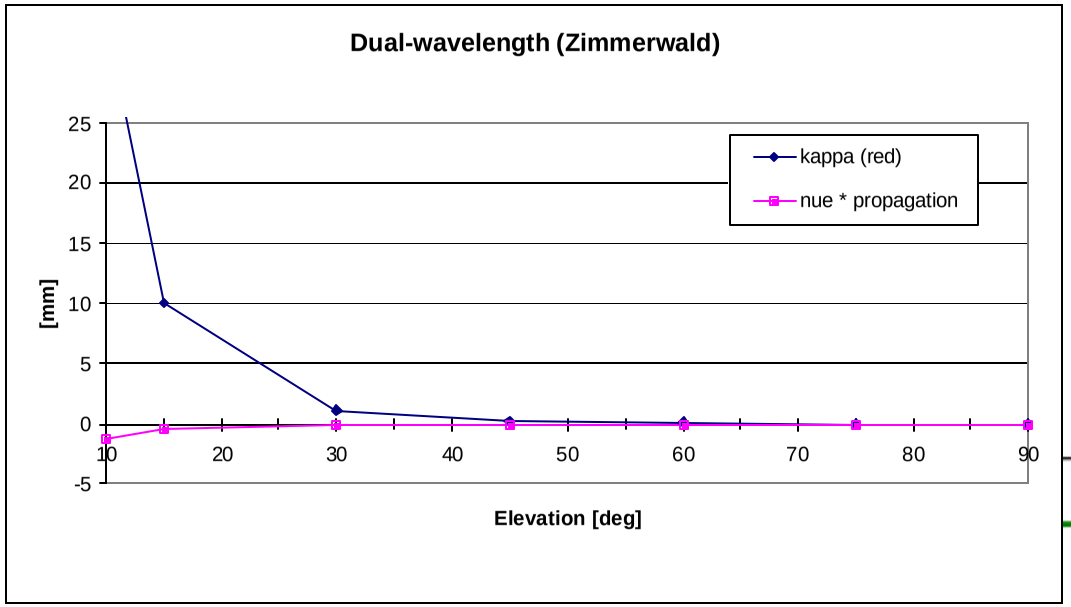

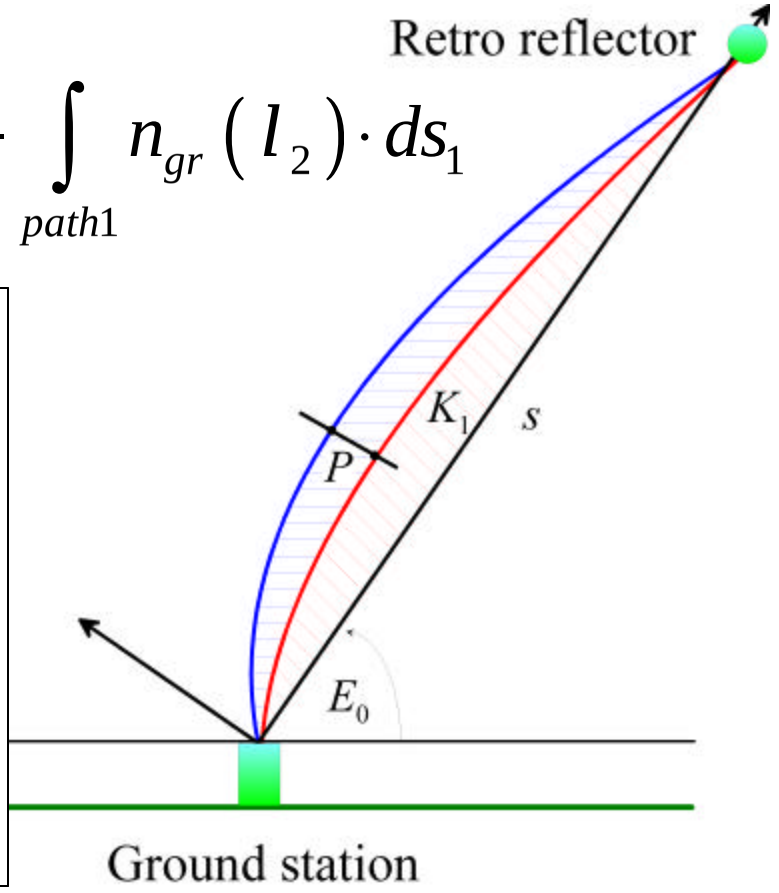

Water vapour range effect (1)

Integrated water vapour $IWV \equiv \int_{path} r_{wet} ds$

Single wavelength $R_w = W(l) \cdot IWV$

Dual-wavelength (Zimmerwald)

$\Delta_{12} R_w = W(l_1) H_{12} IWV$

$H_{12} = 0.42$

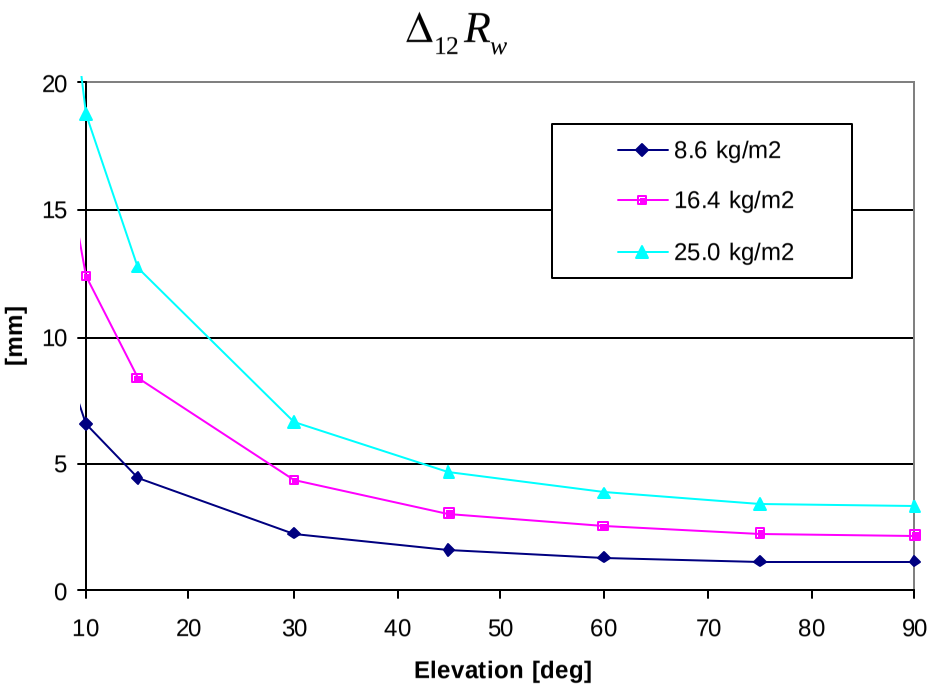

Water vapour range effect (2): Modelling of $\Delta_{12} R_w$

- *IWV* highly variable in position, azimuth and time

Example:
Potsdam
hourly *IWV* values
WVR and GPS

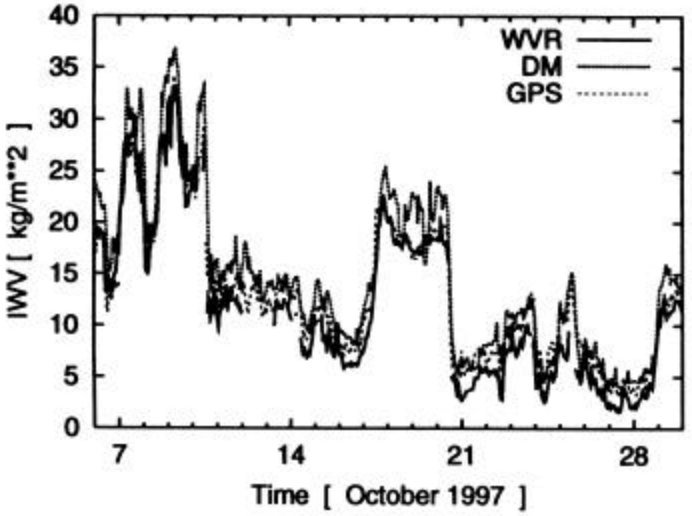

- GPS very useful and readily available technique (5-10% resolution of bias)
- Could be used to estimate the azimuth variation and thus $\int_{path1} r_{wet} \cdot ds_1$

Summary

- Rigorous derivation
- Horizontal gradients eliminated
  except for their effects on K_1 and IWV
- K_1 (10 mm for E_0=15°) can be modelled
- P <1 mm for E_0=15°
- IWV effect (11 mm for E_0 =15°) can be estimated using GPS (azimuthal sectors)

Problems

- Dual wavelength measurements:

  bias, precision, sampling?

  required precision $\simeq$ 0.04 mm
- Effect of turbulence
- Folded path?
- Dispersion precision: absorption bands for n_{gr}?

  required precision $\simeq 10^{-9}$
- Centre-of-mass correction
- Dispersion in glass retro-reflectors?

Using GPS-derived PWV to estimate tropospheric delay

A Combrink & L Combrinck

HartRAO Space Geodesy Programme

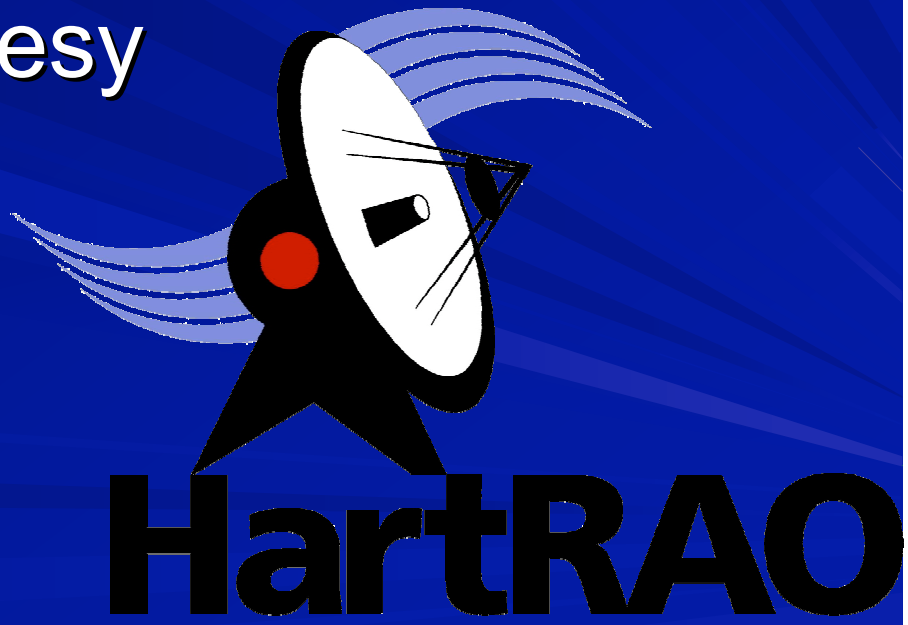

Assumptions

- Ground-measured Relative Humidity is uncorrelated with amount of water vapour in the troposphere.
- Tropospheric delay can be split up into wet and hydrostatic components (as for microwaves).
- Hydrostatic delay proportional to pressure, wet delay proportional to PWV.

Method used (for MOBLAS6)

- Obtain estimated zenith delay (microwave) for HRAO (collocated IGS station) from IGS final product.
- Fit 3rd order polynomial through points to determine zenith delay at SLR normal point observation time.
- Use pressure and temperature measurements with GPS zenith delay to determine (zenith) PWV.

Method used (continued)

- Multiply PWV by refractivity of water to get wet component of zenith delay.
- Use [Marini&Murray minus wet delay] as first approximation of hydrostatic component to obtain constant of proportionality $k(latitude, wavelength, height)$ ($HD = k \times P$)

Note: k should preferably be determined by radiosonde methods.

Method used (continued)

- Processed two years' data for Lageos 1 & 2 – which included 16100 normal points from MOBLAS6
- Used RGODYN (Appleby) which employs the Marini&Murray model.
- Used Marini&Murray model for all other stations.

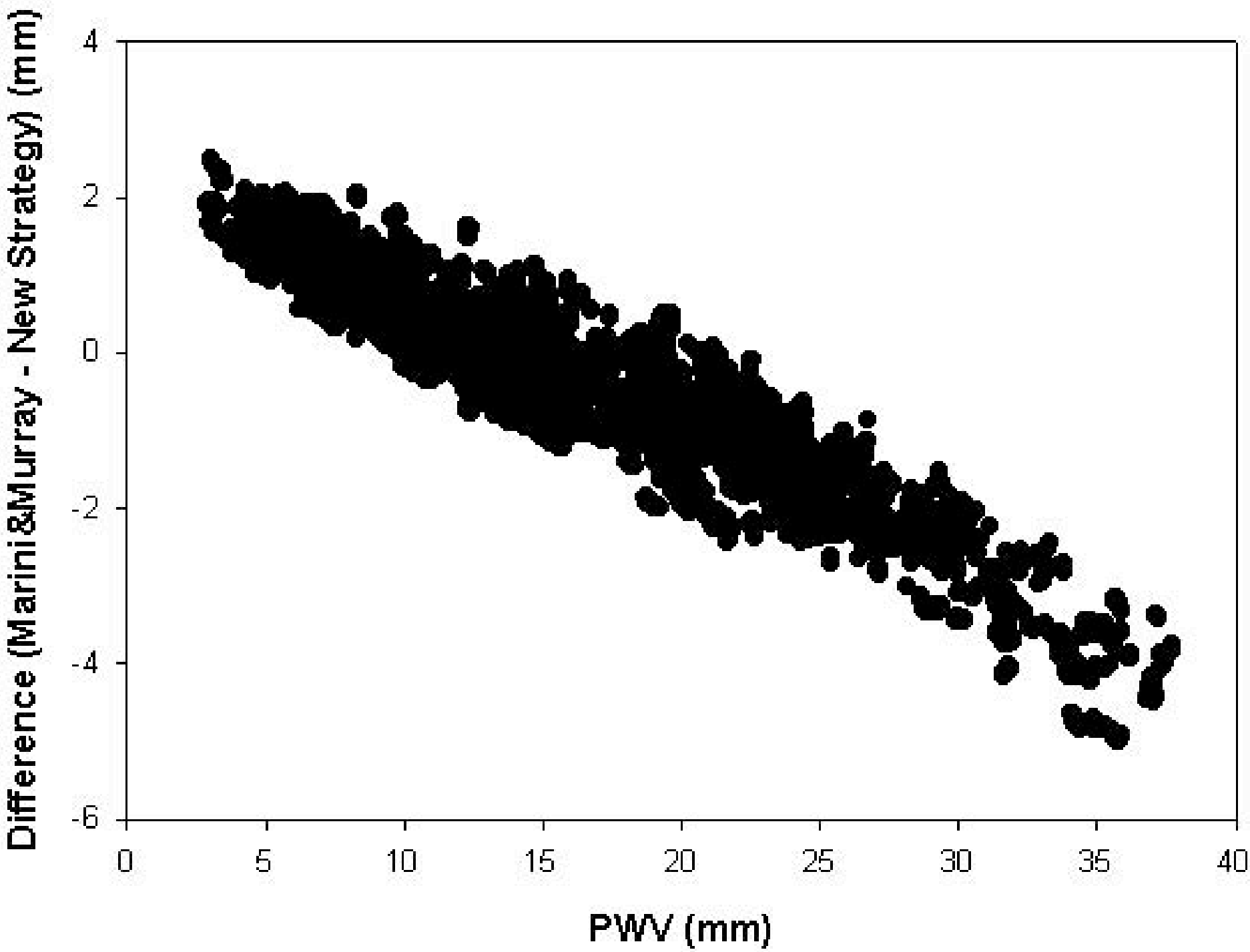
Difference (Marini&Murray - New Strategy) (mm)
4
2
0
-2
-4
-6
0
5
10
15
20
25
30
35
40
PWV (mm)

New Estimate

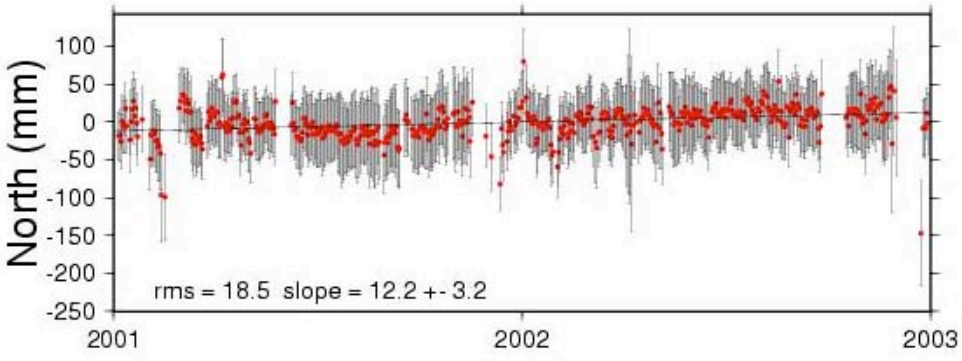

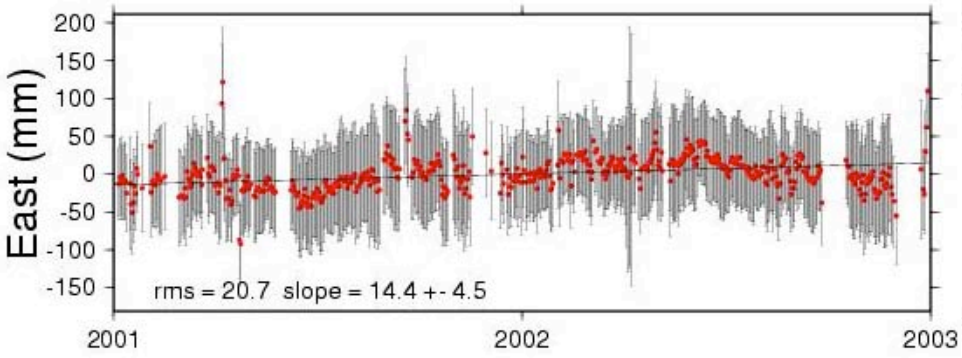

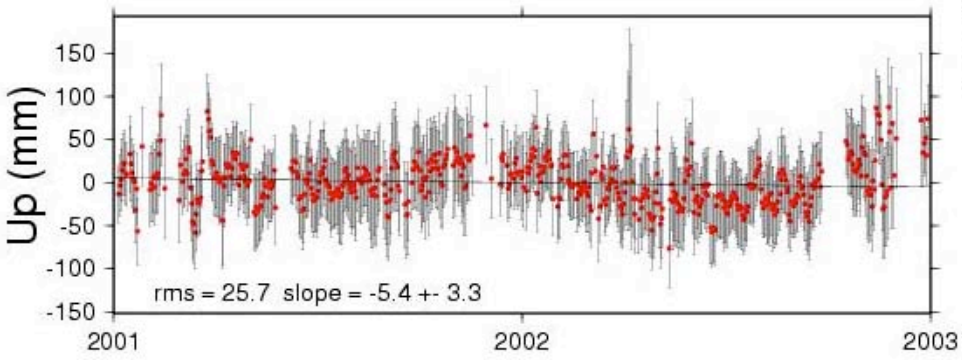

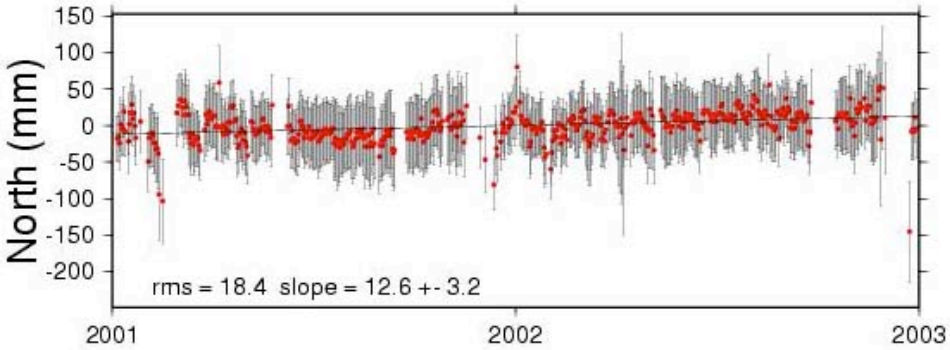

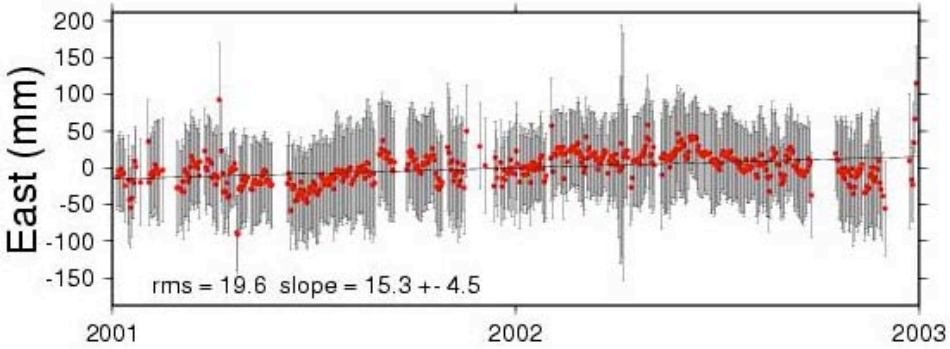

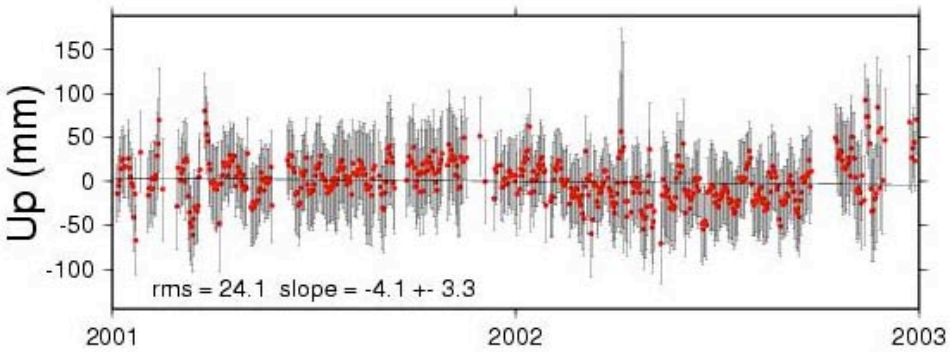

Marini & Murray

Results

- RMS of individual position estimates reduced by 0.5%, 5.3% and 6.2% in north, east and up directions respectively.
- Comparing time series with collocated VLBI: calculated station velocities improved by 10%, 70% and 23% in the north, east and up directions respectively.

Concluding remarks

- Including PWV in tropospheric delay estimation appears to improve results.
- To be done for more stations and over longer time span.
- Determine “constant” k from theory and radiosonde data instead of fitting data to Marini&Murray model (southern hemisphere?)
- Collocation of GPS, using other satellite techniques to estimate PWV at all sites (GPS results include gradients).

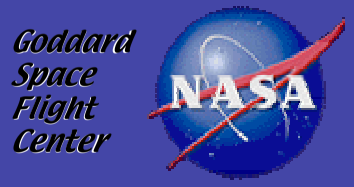

Refraction Modeling Studies in Support of ILRS Data Analysis

Erricos C. Pavlis

Glynn Hulley

JCET/UMBC - NASA/GSFC

2003 ILRS Workshop on Laser Ranging
October 28-31, 2003, Kötzting, Germany

Introduction

- UMBC/JCET is PI for AIRS instrument on NASA's AQUA spacecraft of EOS program
- When the mission is declared operational (real soon!!!), it will provide quick access to global fields of temperature, water vapor, and other geophysical environmental parameters daily in rapid mode
- Such data can be used for improved atmospheric delay modeling (e.g. gradients)

AIRS on AQUA

Illustration of the AIRS/AMSU Field-of-Regard (FOR)

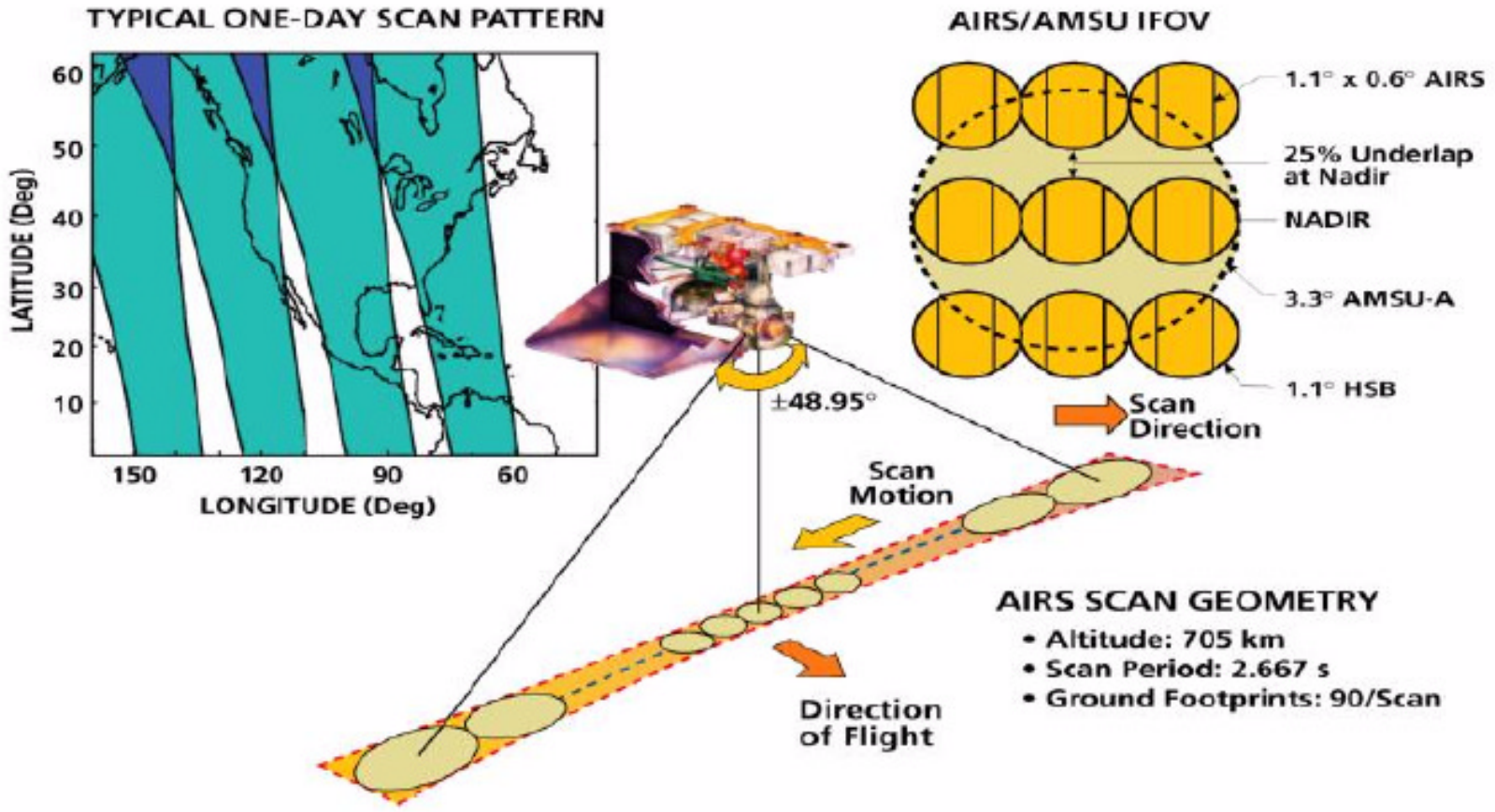

AIRS on AQUA

"First Light over the Med"

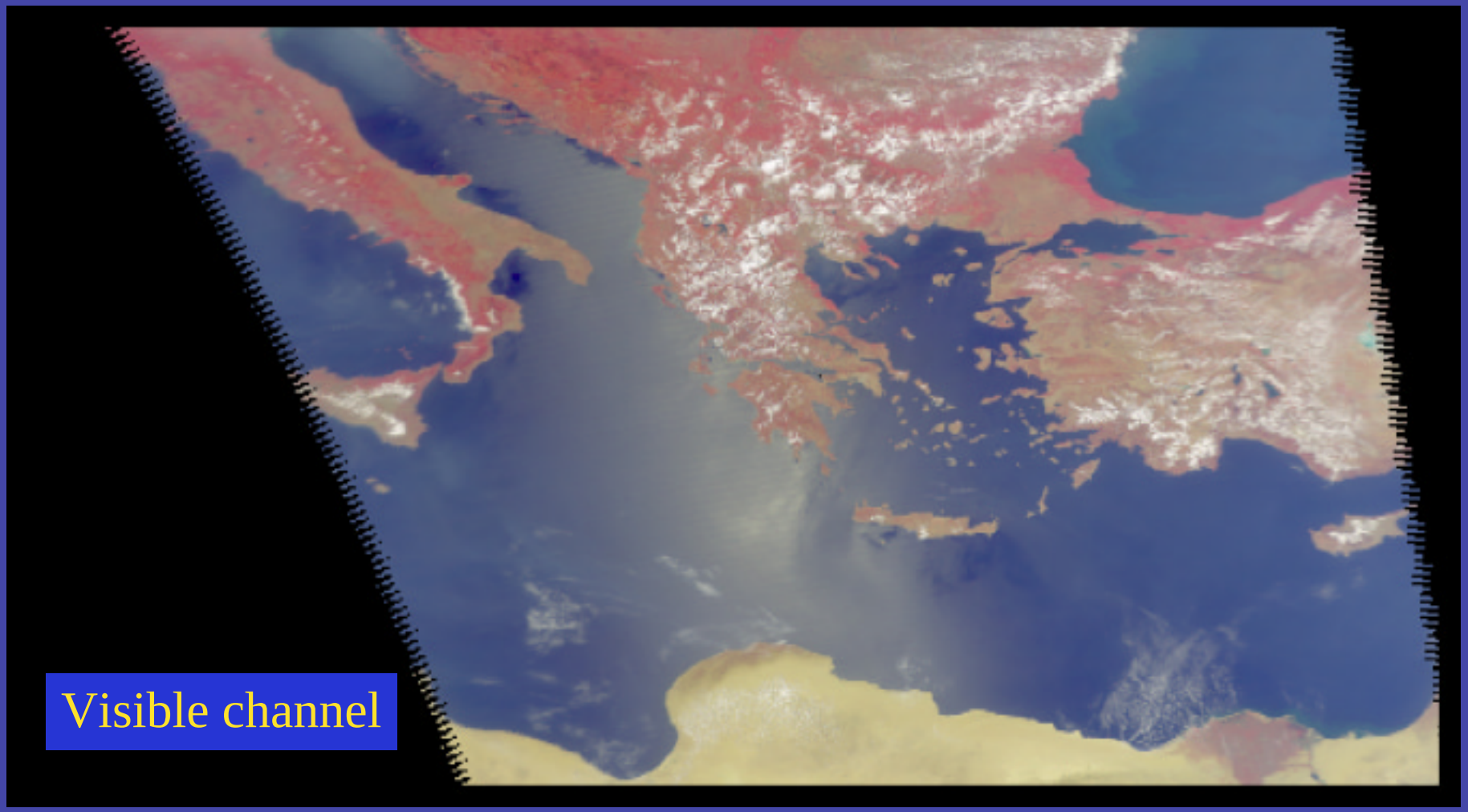

AIRS on AQUA

"First Light over the Med"

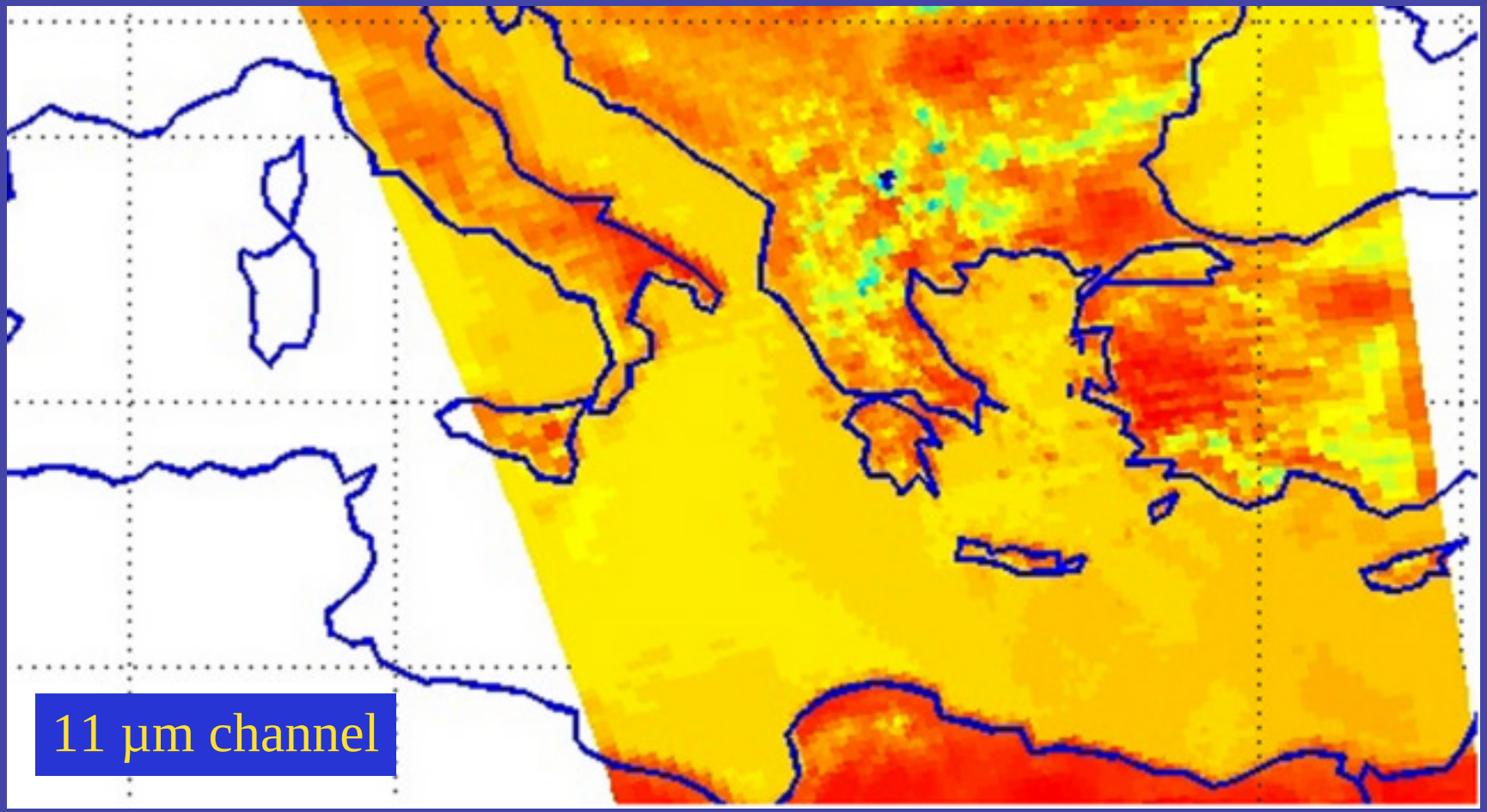

AIRS Products

Summary of Geophysical Products

$T(p)$	vertical temperature profile
$q(p)$	vertical water vapor profile ($\approx$ 8 g/kg @ surface)
$L(p)$	vertical liquid water profile (f/ AMSU/HSB)
$O_3(p)$	vertical ozone profile ($\approx$ 8 ppmv @ 6 mb)
T_s	surface temperature
$\epsilon(\nu)$	spectral surface emissivity, (*e.g.*, 0.95 @ 800 cm^{-1})
$\rho_\odot(\nu)$	spectral surface reflectivity of solar radiation
$P_{\rm cld}$	cloud top pressure for $\leq$ 2 cloud levels
$\alpha_{\rm cld,fov}$	cloud fraction for $\leq$ 2 cloud levels and 9 FOV's
CO_2	total column carbon dioxide ($\approx$ 363 ppmv)
$CH_4(p)$	methane profile ($\approx$ 1.65 ppmv)
$CO(p)$	carbon monoxide profile ($\approx$ 0.11 ppmv)

Ancillary Information Needed for Retrieval

P_s	surface pressure (f/ forecast)
θ	satellite zenith angle
$\theta_\odot$	solar zenith angle
$\epsilon_{\rm cld,\nu}$	spectral cloud emissivity for $\leq$ 2 cloud levels

AIRS Products - Coverage

October 10, 2003

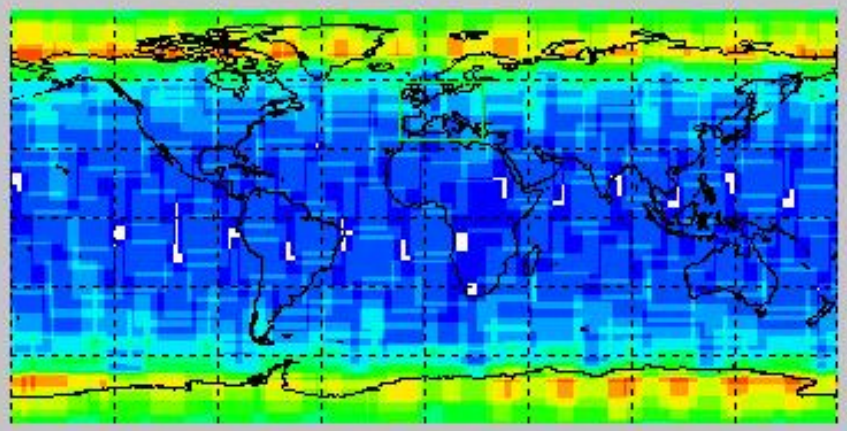

West Longitude	-11.0	South Latitude	34.0
East Longitude	25.0	North Latitude	59.0

ShiftMap

The total number of granules: 241

Color area

Number of granules per area 1 4 7 10 14

AIRS Products - Temperature

October 10, 2003

Goddard Space Flight Center

Channel: Retrieved Skin Surface Temperature

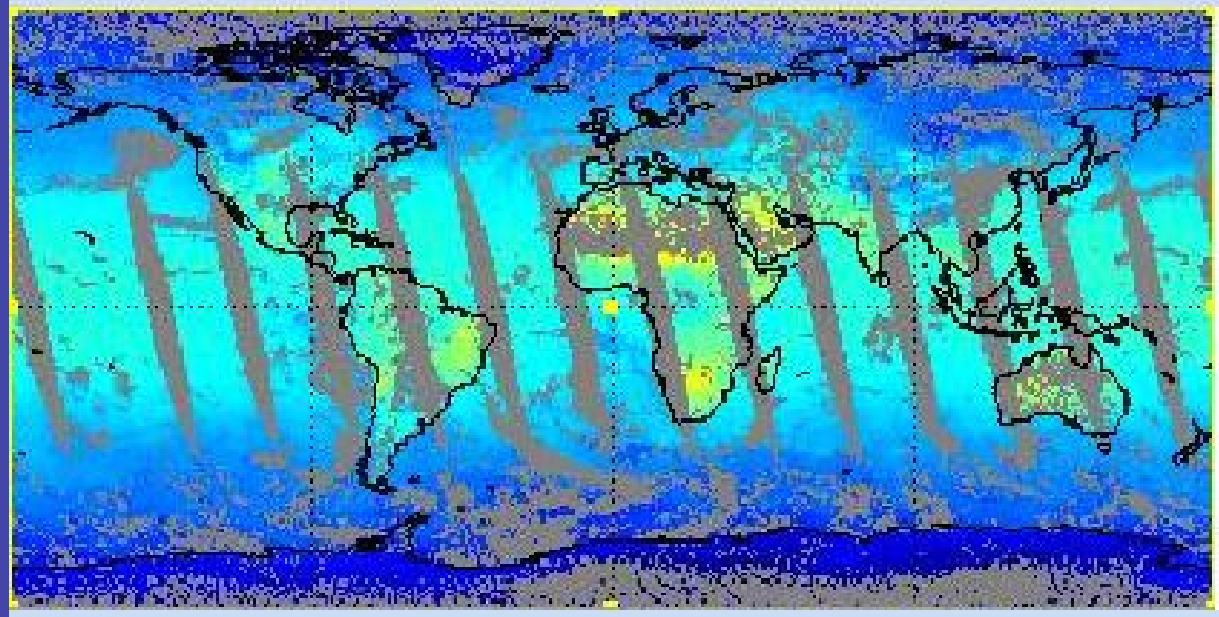

90.0 N

180.0 W 180.0 E

90.0 S

Zoom In Zoom Out

Kelvin

160.0 193.3 226.7 260.0 293.3 326.7 360.0

YEAR: 2003 MONTH: 10 DAY: 10

AIRS Products - Water Vapor

October 10, 2003

Goddard Space Flight Center

Channel: Total Water Vapor Burden

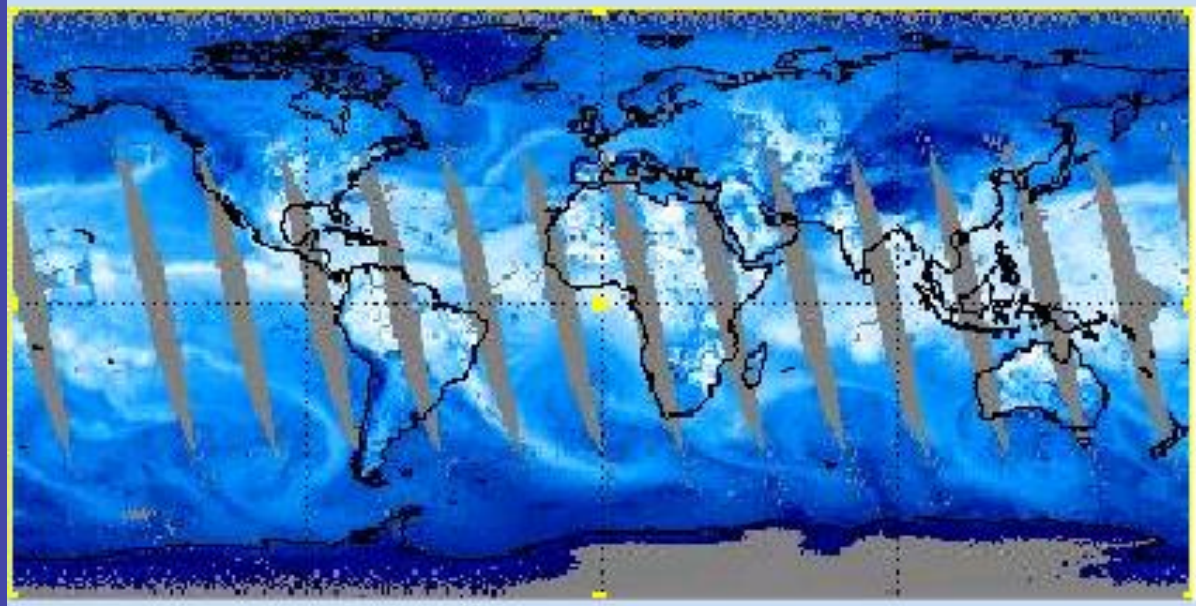

90.0 N

180.0 W 180.0 E

90.0 S

Zoom In Zoom Out

kg/m^2

0.05 16.71 33.37 50.03 66.68 83.34 100.00

YEAR: 2003 MONTH: 10 DAY: 10

H - Gradient Computation

- The system that we are developing in place retrieves the AIRS and ancillary data, several times a day around ILRS sites
- The data are preprocessed and converted to quantities useful in the derivation of the local gradients' functions (G_{NS} and G_{EW})
- The gradient formulation to be adopted is under investigation, including the possibility of an altogether brand new one.

H - Gradient Formulation

A possible model for adoption is one similar to what was used in prior studies with VLBI data:

$$\tau = m(\varepsilon)\cot(\varepsilon)[G_E \sin(\phi) + G_N \cos(\phi)]$$

according to [*Davis et al.*, 1993 and *MacMillan*, 1995]

but other approaches are being examined and in the computations we will adopt the [*Mendes et al.*] mapping function $m(\varepsilon)$, instead of the MTT one.

Summary

- Progress is hindered by incomplete and possibly incorrect data algorithms used in the temperature and WV retrievals and thereby a delay in releasing the data to the community

- JCET has access to a limited number of special (validated) data sets from NOAA, which will be used in the first step for developing, testing and validating this approach.

Atmospheric Refraction at Optical Wavelengths: Problems and Solutions

An update

V. B. Mendes
LATTEX and Departamento de Matemática
Faculdade de Ciências da Universidade de
Lisboa, Portugal (vmendes@fc.ul.pt)

Erricos C. Pavlis
JCET and NASA Goddard Space Flight Center
Univ. of Maryland Baltimore County
Baltimore, Maryland (epavlis@JCET.umbc.edu)

2003 Laser Ranging Workshop
October 28-31, 2003, Kötzting, Germany

Outline

- Background
- Zenith delay models
- Mapping Functions
- Wavelength dependence
- Conclusions

Atmospheric Delay

$$d_{atm} = \int_{ray} (n-1)\, ds + \left[\int_{ray} ds - \int_{vac} ds \right]$$

Propagation Delay

Ray Bending

Atmospheric Delay

$$d_{trop} = d_h^z \cdot m_h(\varepsilon) + d_w^z \cdot m_w(\varepsilon)$$

Hydrostatic Zenith Delay

Hydrostatic Mapping Function

Wet Zenith Delay

Wet Mapping Function

Atmospheric Delay

$$d_{atm} = d^{z}_{atm} \cdot m_t(\varepsilon)$$

Mapping Function

Zenith Total Delay

$$d^{z}_{atm} = 10^{-6} \int_{r_s}^{r_a} N \, dz$$

Zenith Delay Models

- Marini-Murray (1973)
- Saastamoinen (1973) – Hydrostatic and Wet
- Yan and Wang (1999) – Hydrostatic and Wet
- ***Revised version of Ciddor-Mendes – Hydrostatic & Wet***

	P	T	e (RH)	φ	H	λ
MM	✓	✓	✓	✓	✓	✓
SA	✓		✓	✓	✓	✓
YW	✓	✓	✓	✓	✓	✓
CM	✓	✓	✓	✓	✓	✓

Mapping Functions

- Marini-Murray * (1973) – Total **(includes ZD determination)**
- Saastamoinen * (1973) – Hydrostatic and Wet
- Yan and Wang* (1999) – Total
- FCULA (2002) * * – Total (uses surface Temperature)
- FCULB (2002) * * – Total (no meteorogical data)
- FCULZ (2002) * * – as FCULA, **(includes ZD determination with Saastamoinen model)**
  - * Wavelength dependent
  - ** Optimized for 532 nm

Ray-tracing

- Radiosonde data (1998) from a ~180 site global network
- Group refractivity computed according IAG resolutions
- Computer procedures described in Ciddor (1999) and Ciddor and Hill (1999)
- **Compressibility factors computed with full accuracy**
- Water vapor pressure computed using Davis (1992)
- Wavelengths: 355nm , 423nm, 532 nm, 847 nm, 1064 nm

New Zenith Delay Formulation

with Wavelength Dependence

$$d_{atm}^{z} = 10^{-6}\int_{r_s}^{r_a} N\, dz = \int_{r_s}^{r_a}(n-1)\, dz$$

$$d_{atm}^{z} = 10^{-6}\int_{r_s}^{r_a} N_h + 10^{-6}\int_{r_s}^{r_a} N_{nh}$$

Ciddor's 1996 formulation for the refractive index:

$$(n-1) = \left(\frac{\rho_a}{\rho_{axs}}\right)\left(n_{gaxs}-1\right) + \left(\frac{\rho_w}{\rho_{ws}}\right)\left(n_{gws}-1\right)$$

n_{gaxs} is the group refractive index for dry air component

n_{gws} is the group refractive index for water vapor component

New Zenith Delay Formulation

with Wavelength Dependence (cont.)

$$(n-1) = \left(\frac{\rho_a}{\rho_{axs}}\right)\left(n_{gaxs}-1\right) + \left(\frac{\rho_w}{\rho_{ws}}\right)\left(n_{gws}-1\right)$$

Dry air vs. Std. Dry air density ratio

WV vs. Std. pure WV density ratio

Ciddor's 1996 formulation for these ratios involves the use of the compressibility factor of moist air which in earlier implementation was ignored

New Zenith Delay Formulation

with Wavelength Dependence (cont.)

$$Z = 1 - \left(\frac{P}{T}\right)\left(a_0 + a_1 t + a_2 t^2 + \left(b_0 + b_1 t\right) x_w + \left(c_0 + c_1 t\right) x_w^2\right) + \left(\frac{P}{T}\right)^2 \left(d_0 + e_0 x_w^2\right)$$

Z enters the formulation for these ratios in a normalized form which is near unity, but not always:

$$\frac{\rho_a}{\rho_{axs}} = \left(\frac{T_d}{P_d}\right)\left(\frac{Z_d}{Z}\right)\left(\frac{P}{T}\right) - \left(\frac{T_d}{P_d}\right)\left(\frac{Z_d}{Z}\right)\left(\frac{e}{T}\right)$$

$$\frac{\rho_w}{\rho_{ws}} = \left(\frac{T_w}{P_w}\right)\left(\frac{Z_w}{Z}\right)\left(\frac{e}{T}\right)$$

Assessment of Wavelength Dependence of New Model

New Zenith Delay Formulation

ZD from older models vs. Ciddor-Mendes

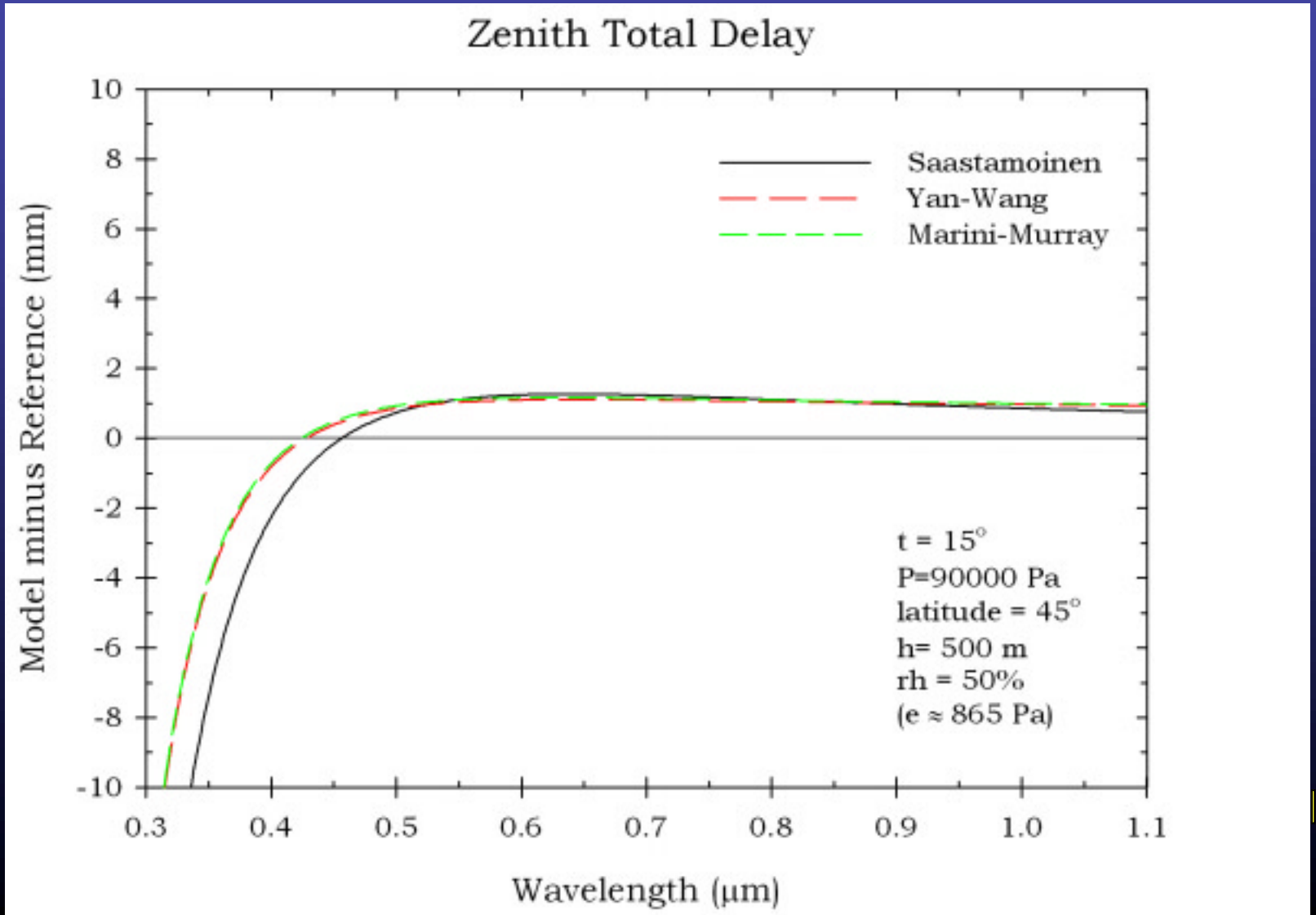

New Zenith Delay Formulation

ZD from older models vs. Ciddor-Mendes

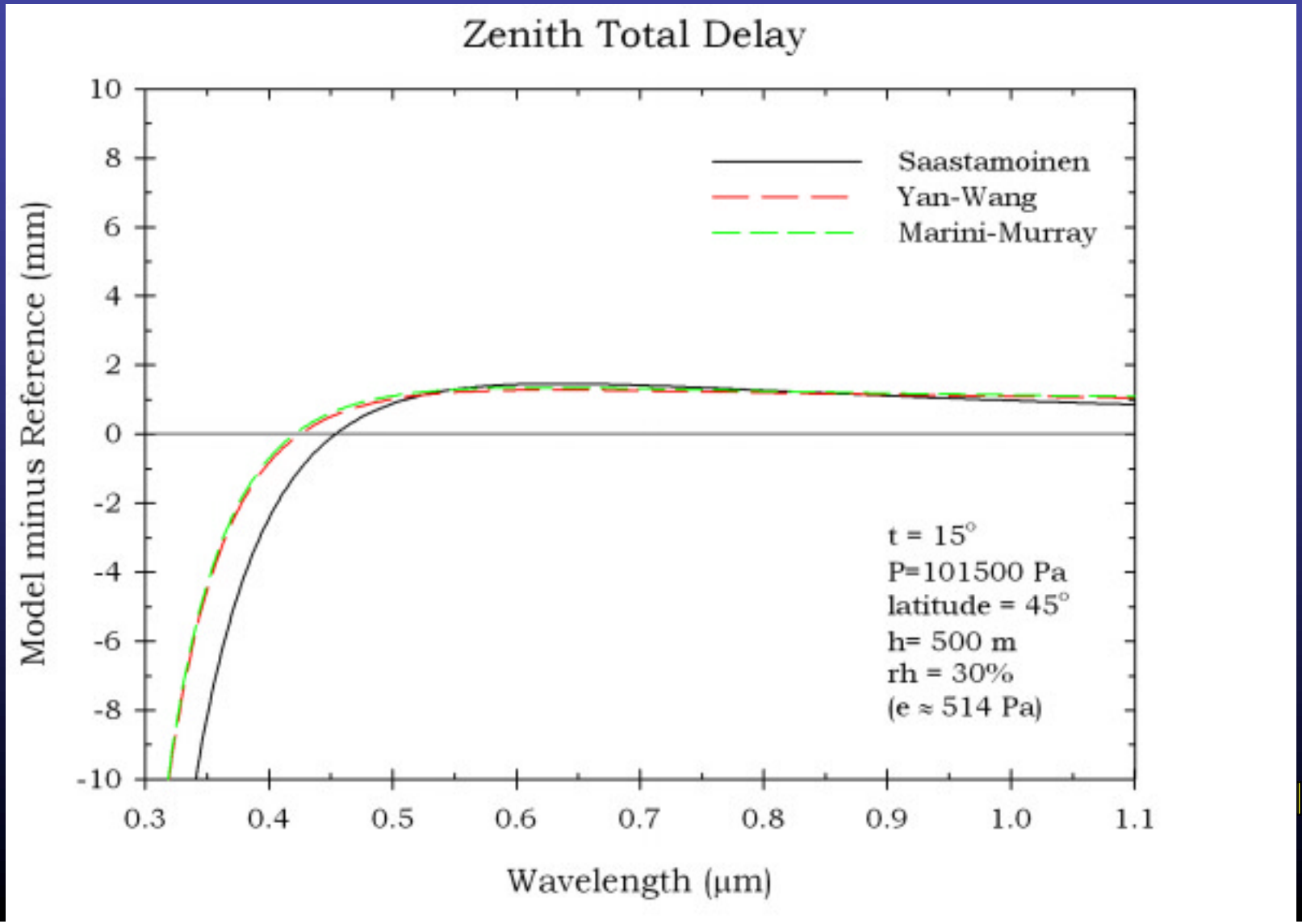

New Zenith Delay Formulation

ZD from older models vs. Ciddor-Mendes

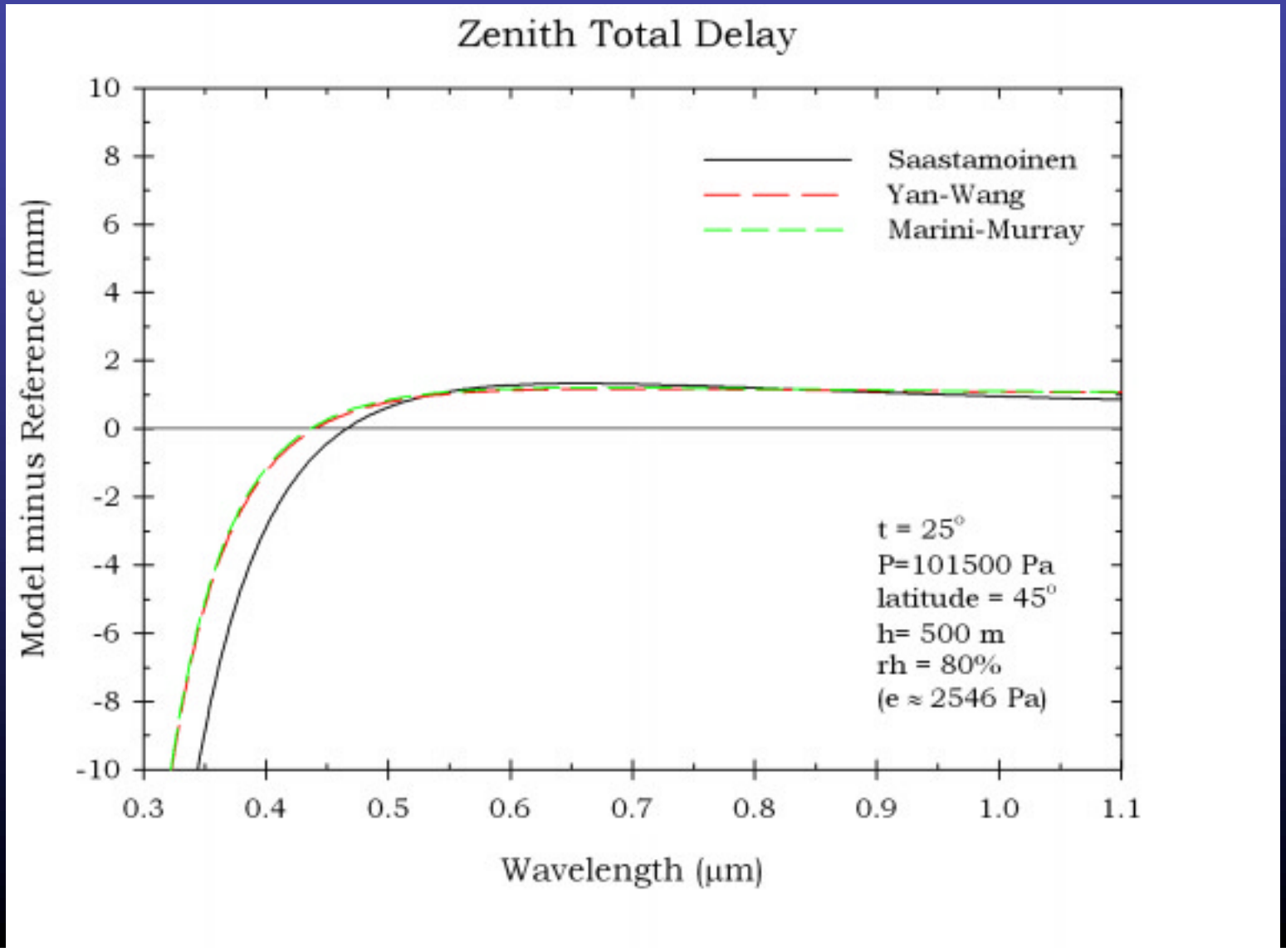

New Zenith Delay Formulation

Radiosonde Comparisons

Marini - Murray

532 nm

694 nm

423 nm

847 nm

355 nm

1064 nm

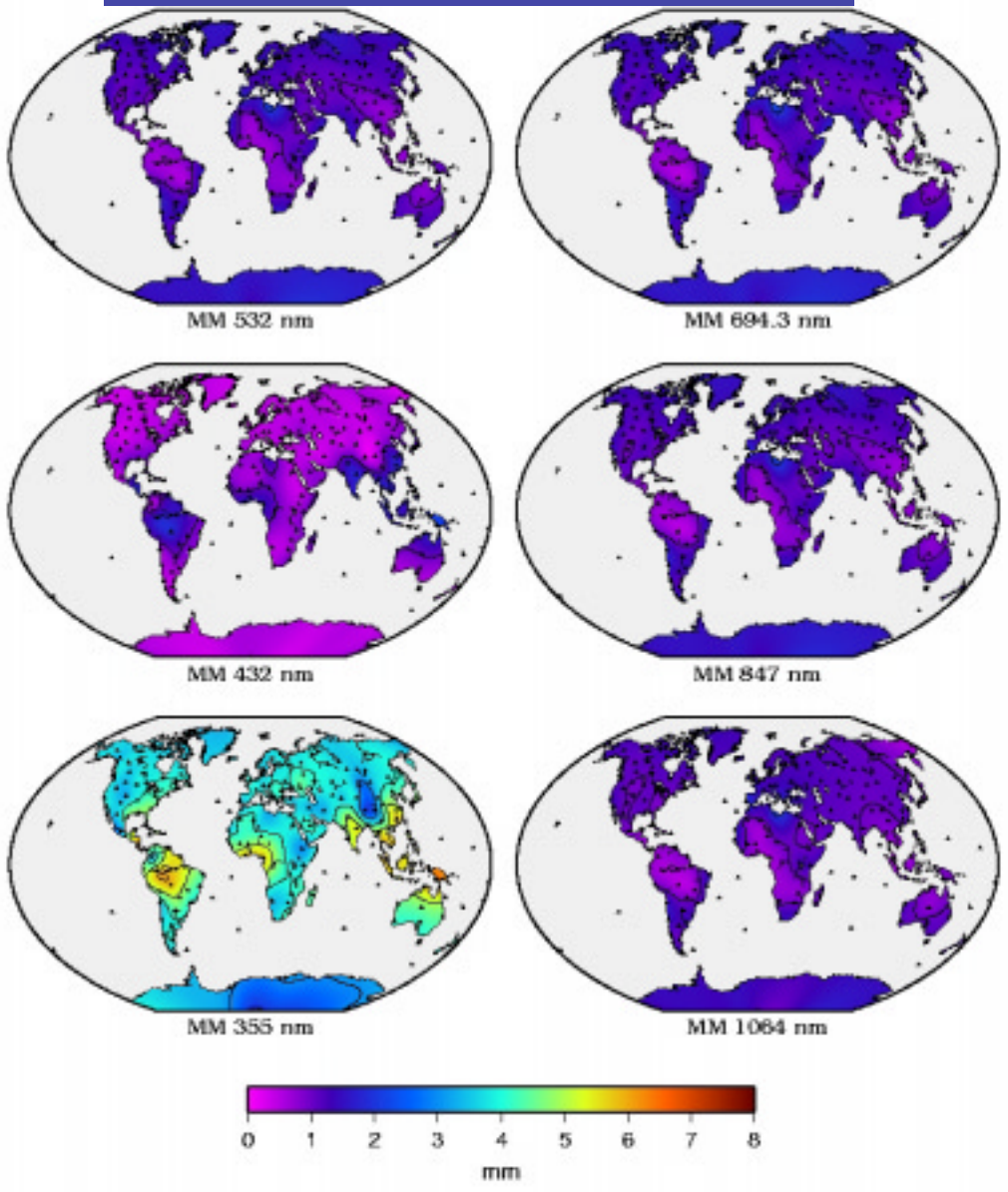

New Zenith Delay Formulation

Radiosonde Comparisons

Saastamoinen

532 nm

423 nm

355 nm

694 nm

847 nm

1064 nm

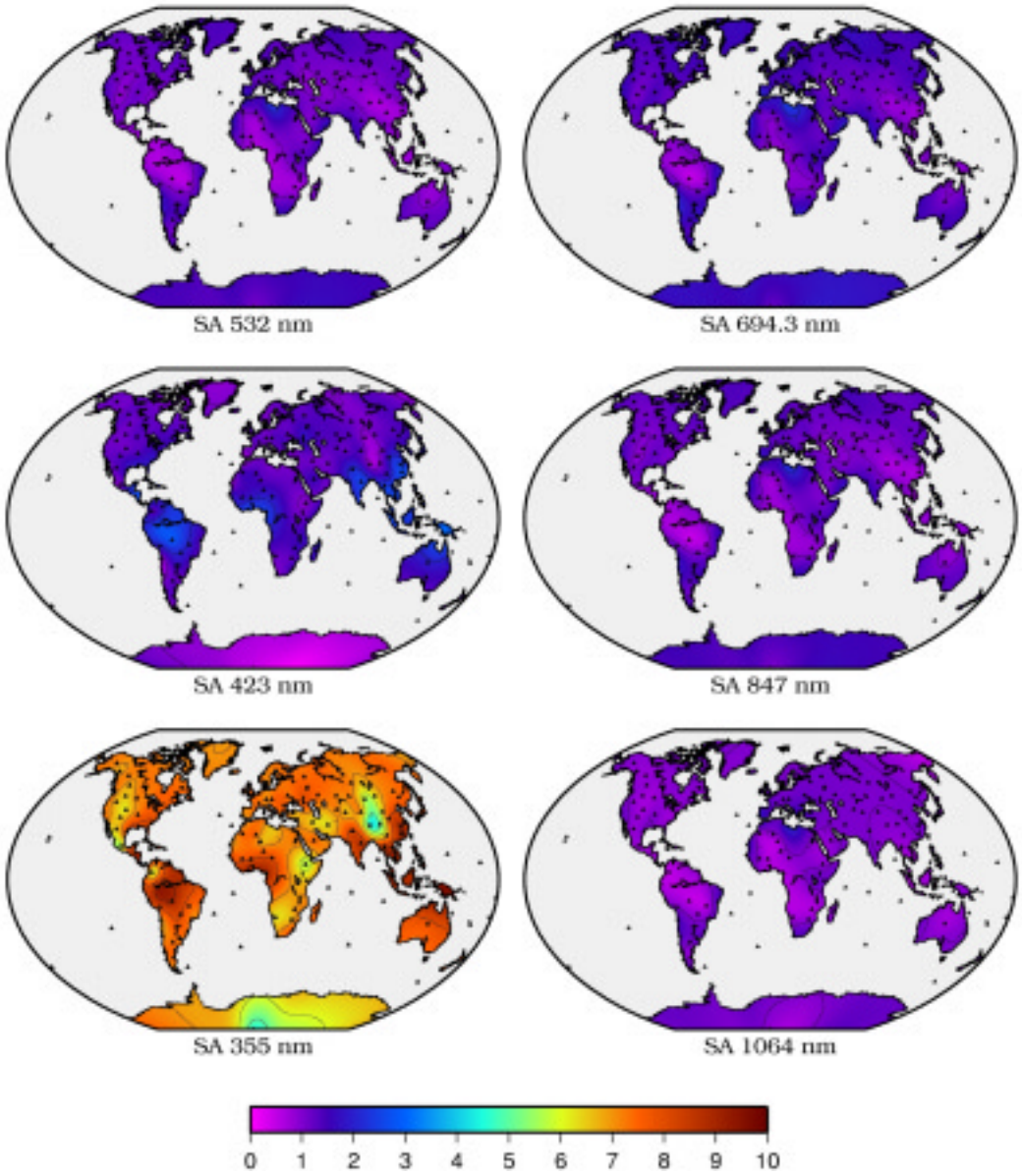

New Zenith Delay Formulation

Radiosonde Comparisons

Ciddor-Mendes

532 nm

423 nm

355 nm

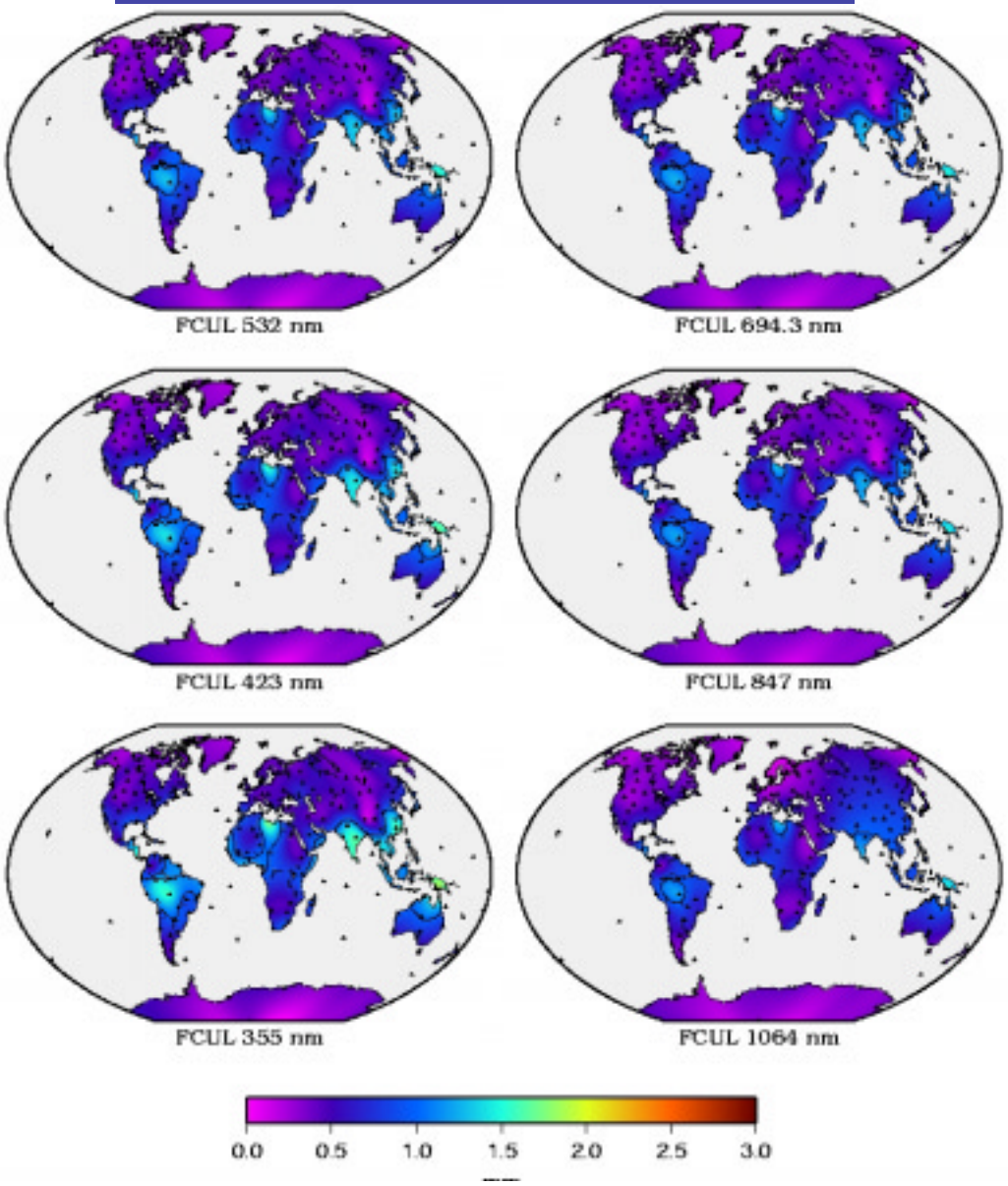

694 nm

847 nm

1064 nm

New Zenith Delay Formulation

Radiosonde Comparisons

Marini-Murray

Ciddor-Mendes

1064 nm

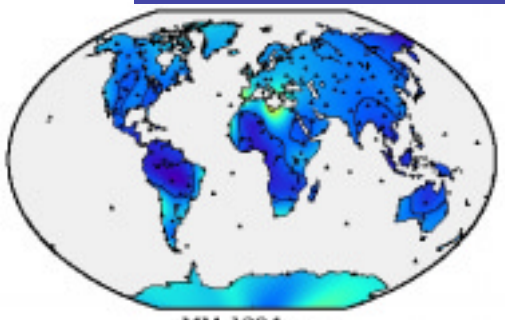

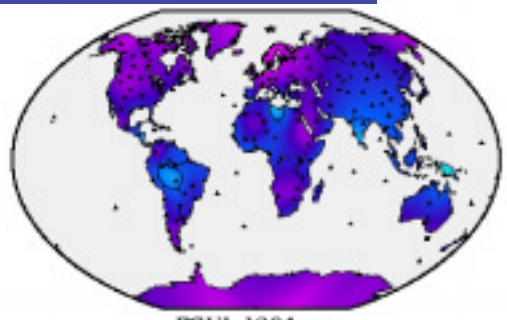

1064 nm

532 nm

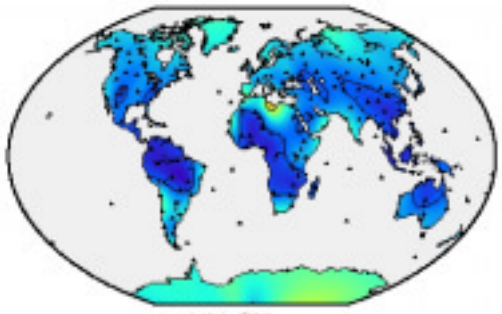

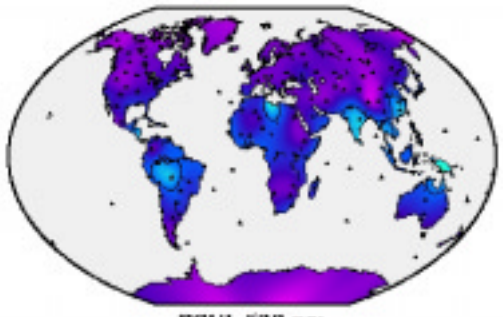

532 nm

423 nm

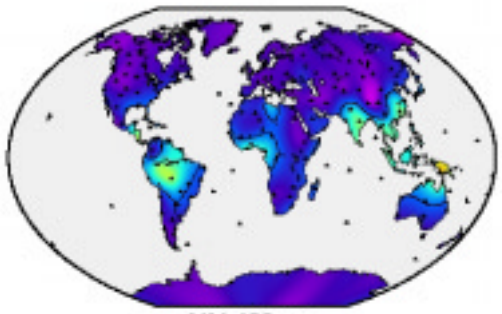

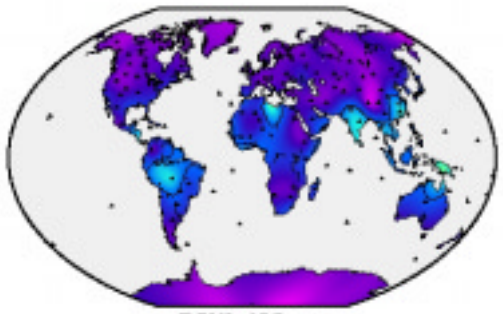

423 nm

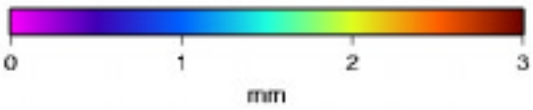

New Zenith Delay Formulation

Radiosonde Comparisons

Saastamoinen

1064 nm

532 nm

423 nm

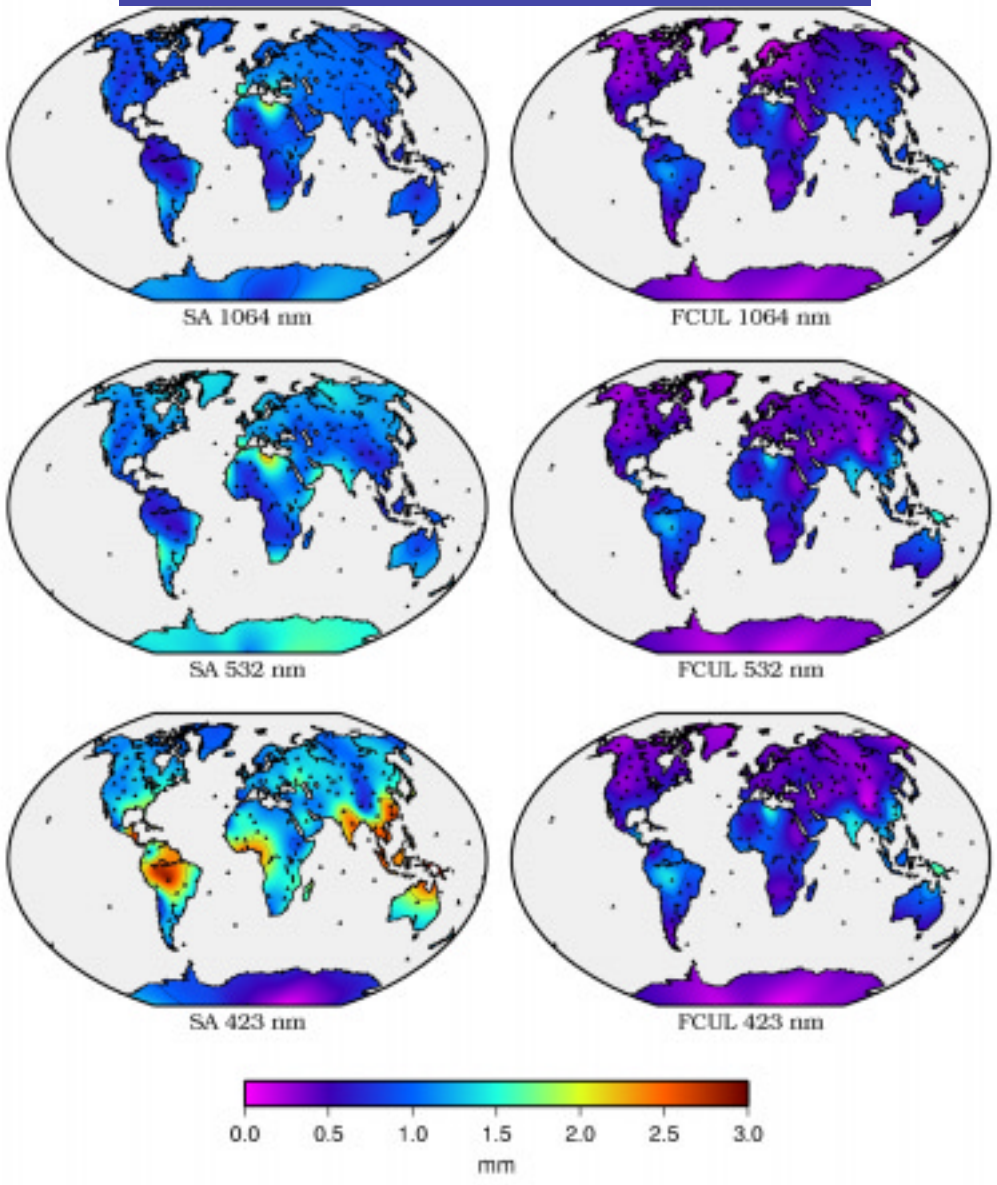

Ciddor-Mendes

1064 nm

532 nm

423 nm

Some concluding remarks ...

- Old zenith delay models exhibit a bias at the ~ 1 mm level for the wavelength interval 500 to 1100 nm (*WRT radiosondes*)
- For wavelengths < 500 nm, the bias changes exponentially, reaching the extreme value of ~10 mm at 355 nm
- The new and old models were compared to a global radiosonde data set (1 yr) and the conclusions are:
  - M-M shows a variable behavior, with best performance around the 423 nm wavelength, worst at 355 nm
  - **Saastamoinen is particularly poor at 355 nm, reaching 10 mm !**
  - C-M (**new**) shows a fairly uniform behavior across the specrum
  - With mapping function performance degrading with increasing zenith angles, these errors will be greatly enhanced in these cases
- SLR testing with low elevation data is in progress, but **PLEASE, observe LOW and release data you may have at wavelengths other than the green !!!**

Atmospheric contribution to the SLR jitter

I.Procházka, K.Hamal, L. Kral, J.Mulacova

Czech Technical University in Prague,

G.Kirchner, F.Koidl

Satellite Laser Station, Graz, Austria

presented at

International Laser Ranging Service Meeting, Koetzting, October 28-30, 2003

Goals:

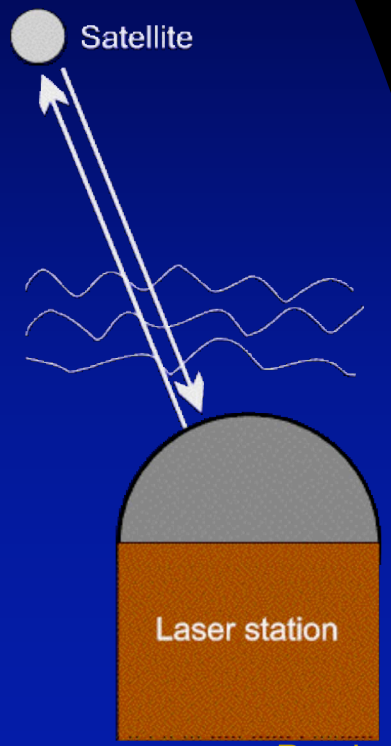

- Evaluate the contribution of the atmosphere fluctuations to the overall SLR jitter budget
- Create and test a model of propagation of a picosecond laser pulse through atmosphere in Satellite Laser Ranging (SLR)
- Verify the model on existing laser ranging data
- propose new laser ranging experiments to verify the model

Motivation

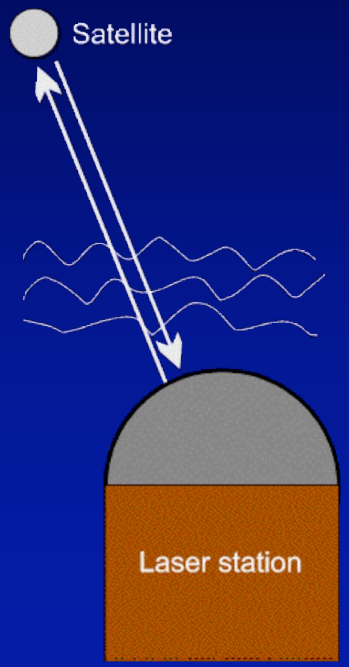

- The observed discrepancy in laser ranging precision (jitter) for different path length and geometry
- atmospheric fluctuation is one of the probable sources of random error contributors

Prochazka,Hamal, Kral,Mulacova,Kirchner, Koidl,ILRS, Koetzting, Oct.28-31, 2003

Geometrical Optics Approach

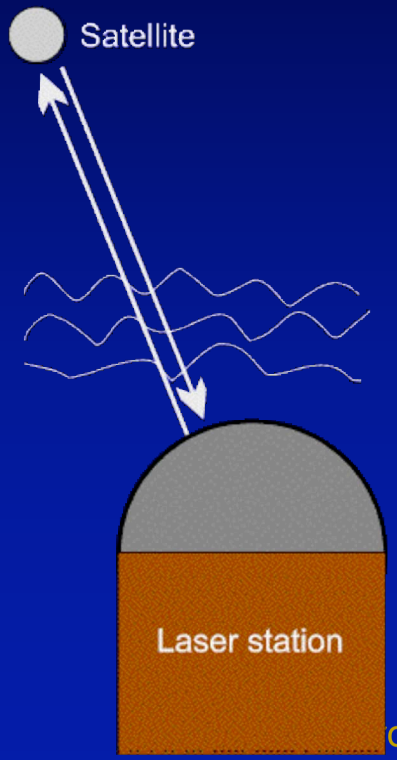

- C. Gardner [(1)] derived analytical formula for mean-square pathlength fluctuation (mm ..cm)

- $< \Delta L^2 > = 26.31\ C_n^2(0)\ L_o^{5/3}\ L_e$

  (Greenwood-Tarazano spectral model used)

- $C_n^2(0)$ ... initial value of refractive index structure constant (turbulence strength at start)
- new estimates of C_n^2 available since '76
- L_o ... outer scale of turbulence
  L_e ... effective pathlength (weighted by $C_n^2(\Delta)$)

(1) C. S. Gardner, Effects of random path fluctuations on the accuracy of laser ranging systems, Appl.Opt. Vol.15, No.10, pp.2539–2545, 1976

Geometrical Approach - Effective Pathlength

$$L_e = \frac{1}{C_n^2(0)} \int_0^L C_n^2(\xi) d\xi$$

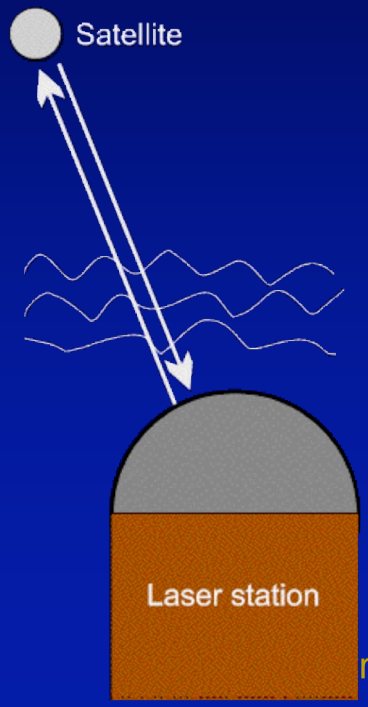

- L ... distance to target
- **Horizontal path:**
  C_n^2 constant ⇒ $L_e = L$
- **Slant path to space:**
  Hufnagel-Valley model of C_n^2 height dependence used to evaluate L_e

Geometrical Approach - Slant Path to Space

- atmospheric mass influence,
- ranging jitter dependence on the zenith distance and station elevation above the sea level

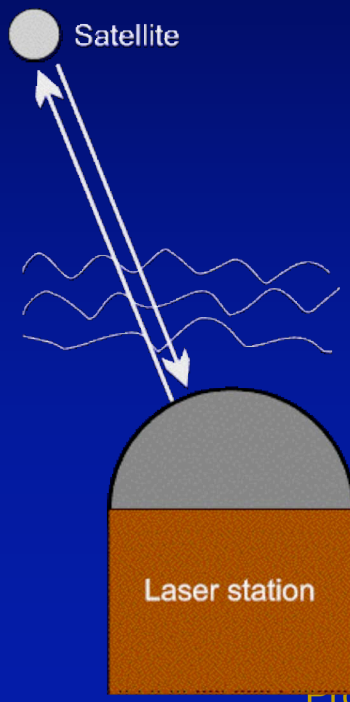

station at a sea level

elevation 2000 m above the sea level

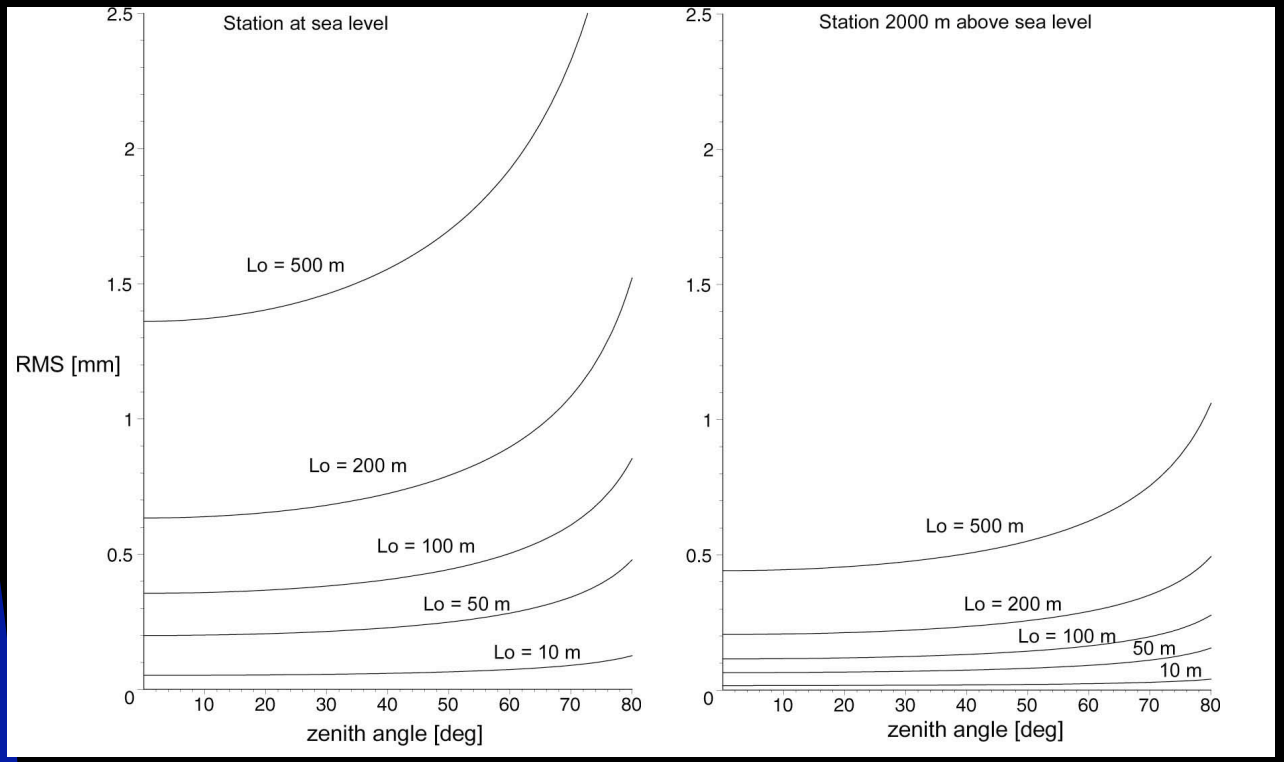

Experiments at SLR Graz

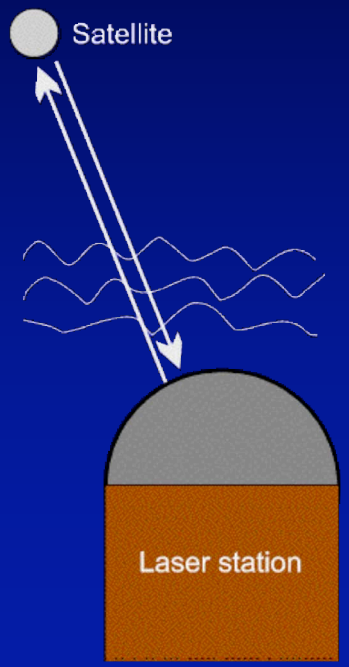

- horizontal path
  - laser ranging / 2 kHz reprate, 1 mm rms/
  - seeing measurements / via CCD, 30 msec time res./
- slant path
- SLR

Experiment - seeing versus ranging jitter

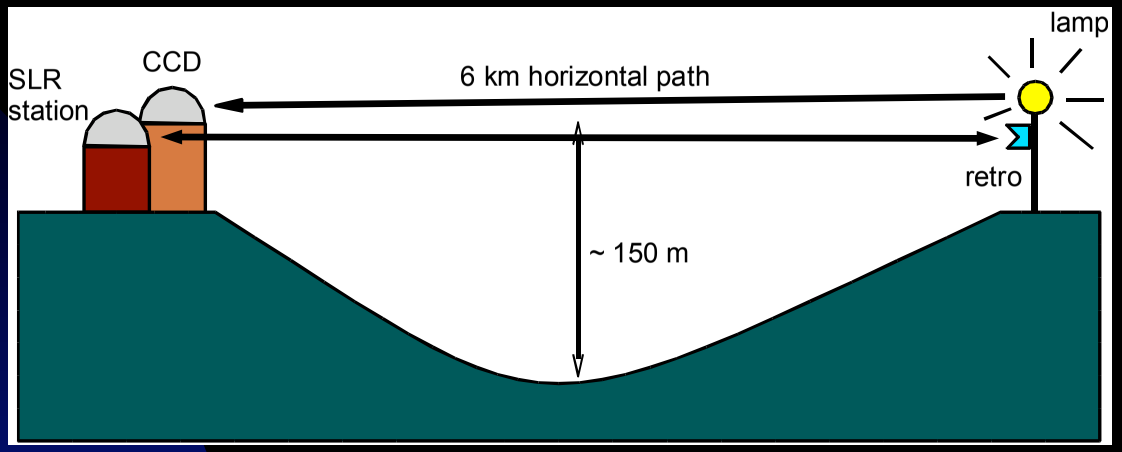

- MEAD 20” telescope
- CCD Star Tracker with image processing SW
- geometry resolution 0.8 ‘’ / pixel
- direction resolution 0.01 ‘’
- integration time 30 - 100 ms

Experiment - horizontal seeing results

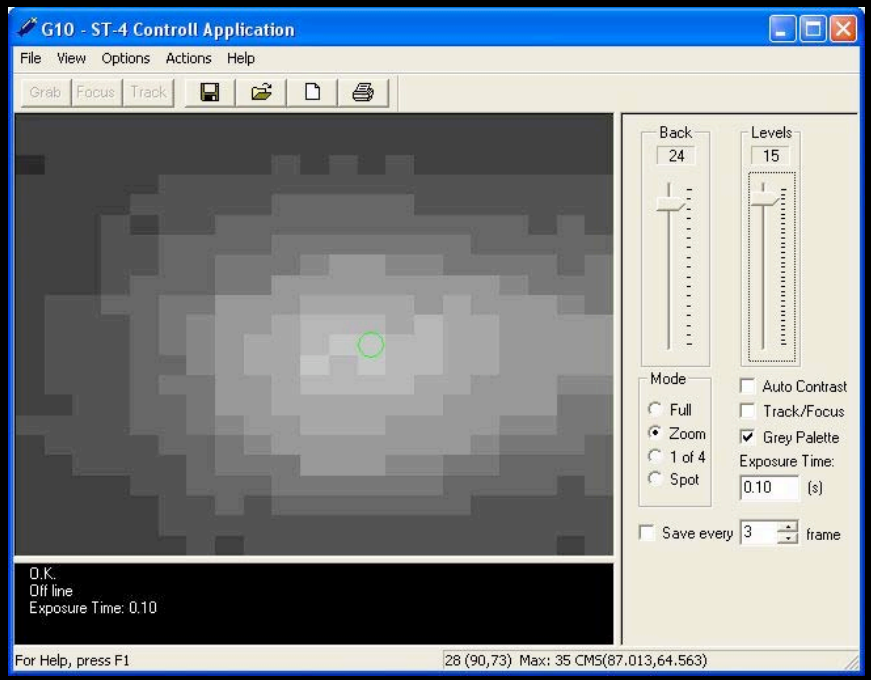

direction fluctuations

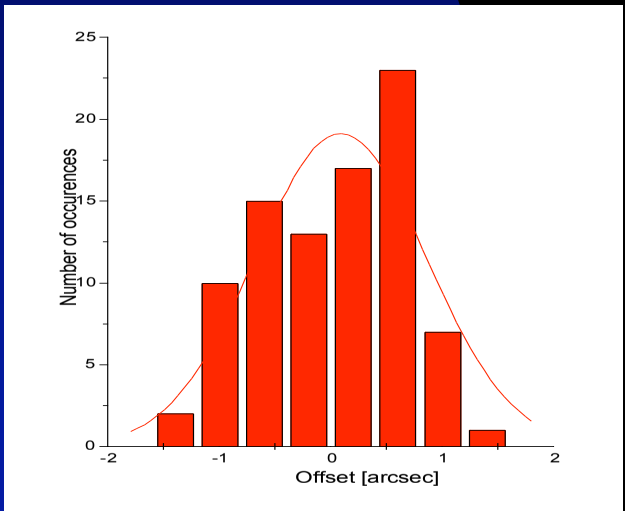

arc seconds

- FWHM = 1.9 arc sec
- equal for both 30 and 100 ms integration

Prochazka,Hamal, Kral,Mulacova,Kirchner, Koidl,ILRS, Koetzting, Oct.28-31, 2003

Horizontal path laser ranging

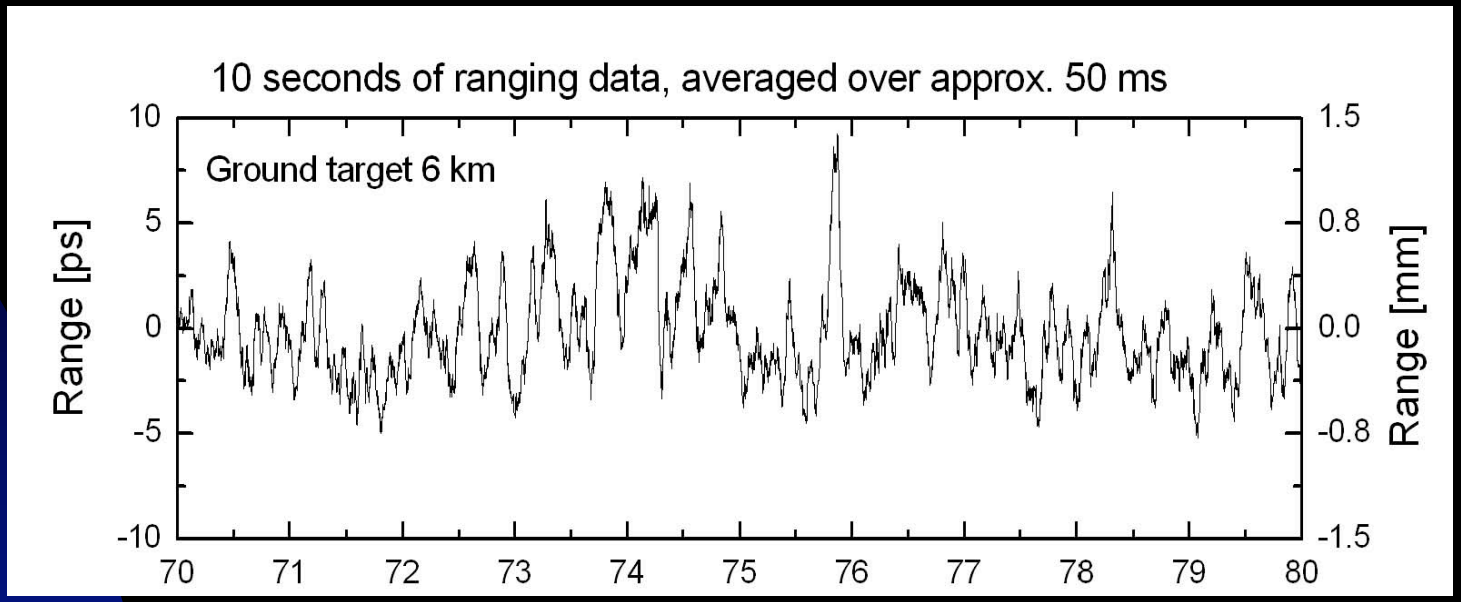

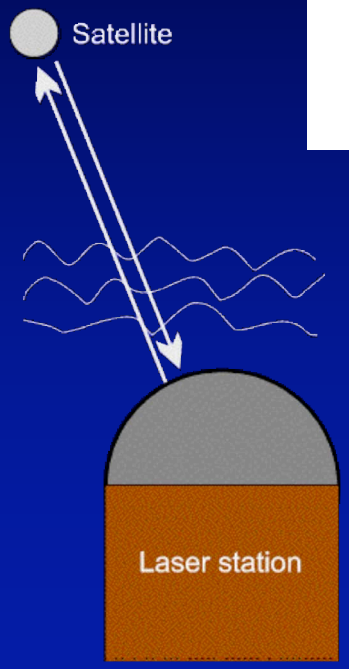

- single shot precision ~ 1 mm RMS
- displayed moving average /50 ms in time/
- main fluctuation time constant ~ 130 ms
- atmospheric fluctuation induced ranging jitter ~ 0.4 mm

- well correlates with the horizontal seeing data and model by Gardner

Prochazka,Hamal, Kral,Mulacova,Kirchner, Koidl,ILRS, Koetzting, Oct.28-31, 2003

Satellite laser ranging, ERS 2, Envisat

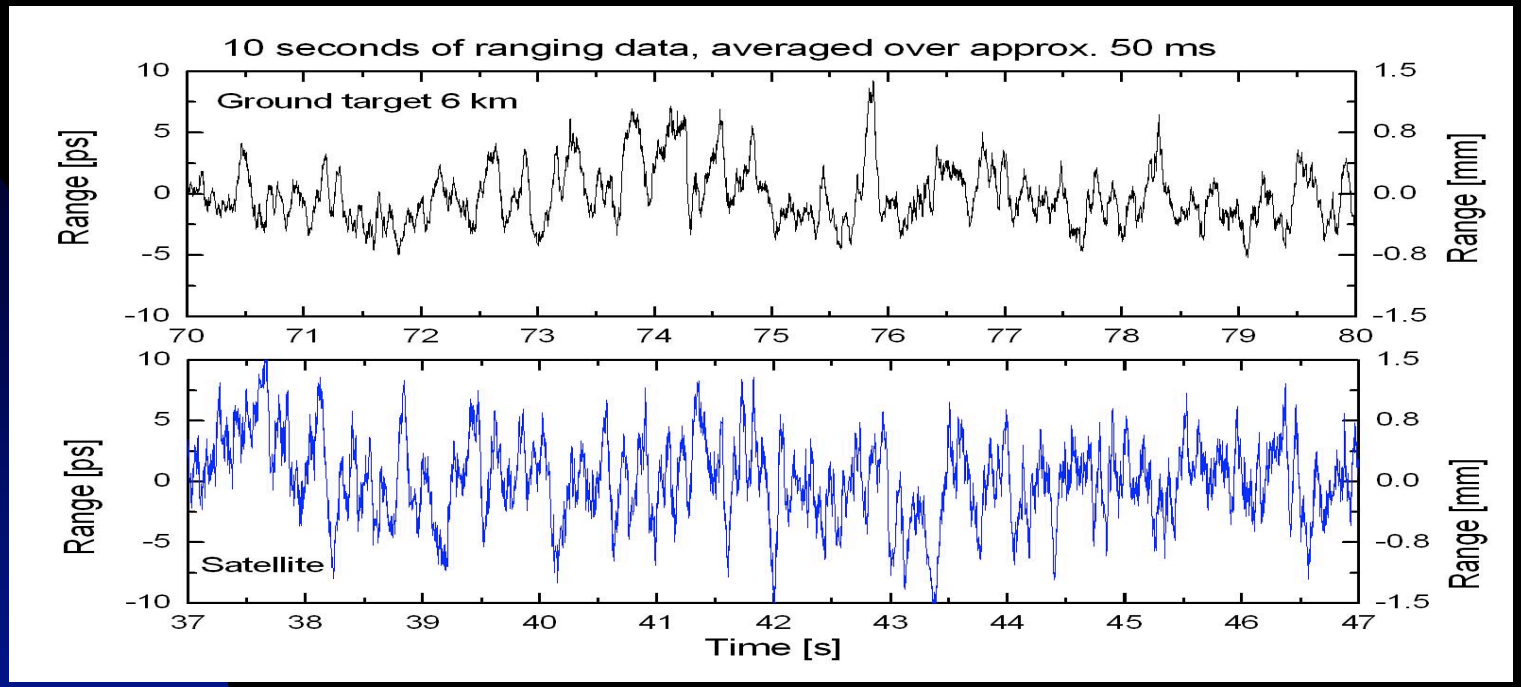

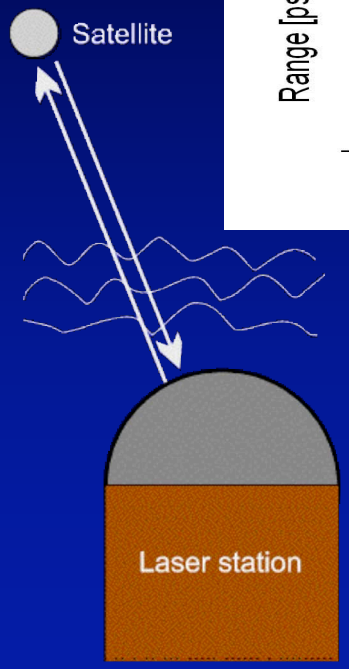

- single shot precision 2.8 mm RMS
- the time structure is less pronounced, 130 ms characteristic time may be identified
- the amplitude is similar to 6 km ground target

Prochazka,Hamal, Kral,Mulacova,Kirchner, Koidl,ILRS, Koetzting, Oct.28-31, 2003

Conclusion

Low Elevation Survey

Station	Limitation	Success	Comments
Arequipa	20	N/A	mountians mask at 6 degs + safety/security at 20 degs
Beijing	5	5	can go down to 5 degs (mountains at this elevation)
Borowiec	20	N/A	structural (az dep.), signal strength
Changchun	<10	??	can range down to 5 degrees assuming enough signal strength
Concepcion	18	11	have tracked LAGEOS down to 11 degs, safety limit is 18 degs
FTLRS	15	??	15 degs for LEO and 30 degs for LAGEOS
Golosiiv	15	??	can range down to 15 degs in certain azimuths
Grasse	5	5	**Closed**
Grasse (LLR)	5	5	can track LAGEOS and high sats. down to 5 degs
Graz	5	5	can range down to 5 degrees
Greenbelt	10	TBD	**approved for down to 10 degs, approval for other NASA sites pending**
Haleakala	20	N/A	structural interference from our dome at 20 degs
Hartebeesthoek	10	??	mountians mask as 10 degrees
Herstmonceux	30	N/A	only track down to 30 degrees for safety reasons
Katsively			**no response**
Koganei (CRL)	15	??	trees and buildings at 15 degrees
Komsomolsk			**no response**
Kunming	15	15	can track down to 15 degs
Lviv	20	N/A	structural limitations at 20-25 degs
Maidanak 2			**no response**
McDonald	20	N/A	need safety approval and HW/SW and structurl limitations
Metsahovi2	8	??	Some satellites to 8 deg., not Lageos or Jason
MLRO	20	N/A	safety and hardware/software issues below 20 deg
Monument Peak	20	N/A	safety, hardware/software
Mt. Stromlo2	15	??	site limit of 20 degs, perhaps can get approval at 15 degs
Potsdam	30	N/A	trees
Potsdam3	20	12	have gotten LAGEOS returns down to 12 deg, safety restrictions at 20 degs
Riga	15	??	can range down to 12 degs in the North, 18 degs other directions, 30 degs for LAGEOS
Riyadh	20	N/A	safety, hardware/software issues, system physical limit is 2 degs
San Fernando	0	??	no known physical or site mask limitations
Shanghai	25	N/A	25 degrees at current location
Shanghai, new site	0	N/A	can range to the horizon at new location
Simeiz	10	<15	can track down to 10 to 15 degs, but not LAGEOS
Simosato	15	15	can range down to 15 degrees, below 15 there are safety issues
Tahiti	20	N/A	safety, hardware/software
TROS-China	3	??	can range down to 3 degrees, signal strength limitations
Wettzell	10	N/A	safety limit is 20 deg, system capability is 10 degs
Wuhan			**no response**
Yarragadee	15	N/A	airspace current limit is 15 degs, can perhaps go lower
Zimmerwald	10	yes	horizon mask varies between 0 and 20 degs